

Title: Nuclear binding and the light quark masses – Dynamics and constraints

Date: Jul 17, 2008 02:40 PM

URL: <http://pirsa.org/08070028>

Abstract: I will describe a method of understanding how the nuclear binding energies depend on the masses of the light quarks. This is useful in applications ranging from anthropic constraints to equivalence principle tests and bounds on the time variation on the quark masses.

Nuclear binding and light quark masses: Dynamics and constraints

Advertisement: (OT) Limits on spatial variation of Λ ... from CMB

with Evan
Donoghue

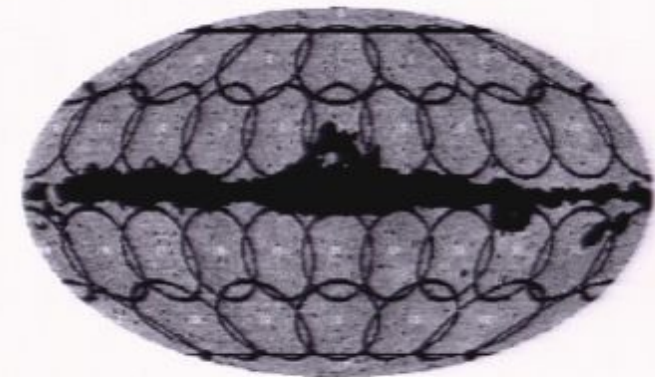
Main talk

- 1) Nuclear binding –heavy nuclei
 - 2) Quark mass dependence
 - 3) Anthropic constraints on quark masses
 - 4) Oklo constraint (very rough and preliminary)
 - 5) Equivalence principle (sketchy)
- 4 papers on related topics**
- 2 solo
2 with Thibault Damour
(one still virtual)

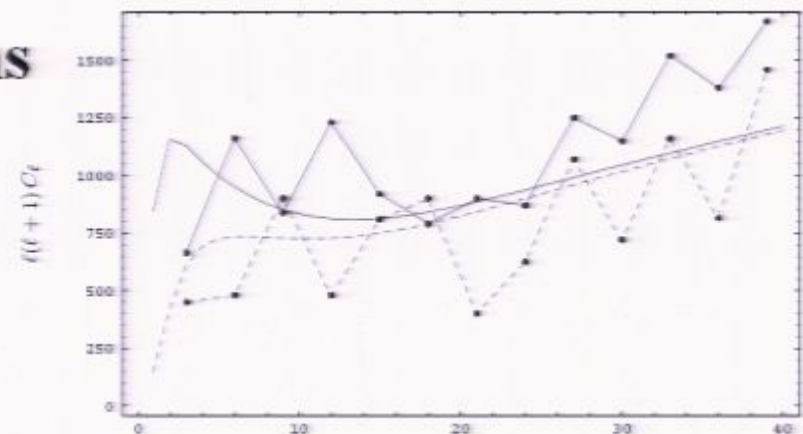
Advertisement: Limits on spatial variations from CMB

with Evan Donoghue

- Eriksen et al demonstrate potential asymmetry in CMB power spectrum
 - stable, $\sim 3\sigma$
 - occurs in low ℓ data – up to $\ell \sim 40$



- Can this be due to spatial variations of some parameters?**
- especially cosmological constant?



Nuclear binding and light quark masses: Dynamics and constraints

Advertisement: (OT) Limits on spatial variation of Λ ... from CMB

with Evan
Donoghue

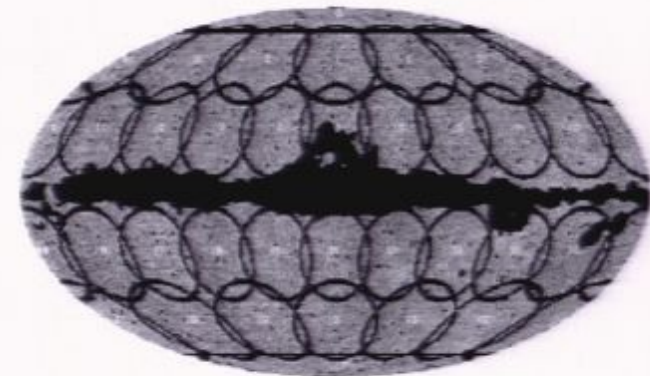
Main talk

- 1) Nuclear binding –heavy nuclei
- 2) Quark mass dependence
- 3) Anthropic constraints on quark masses
- 4) Oklo constraint (very rough and preliminary)
4 papers on related topics
2 solo
2 with Thibault Damour
(one still virtual)
- 5) Equivalence principle (sketchy)

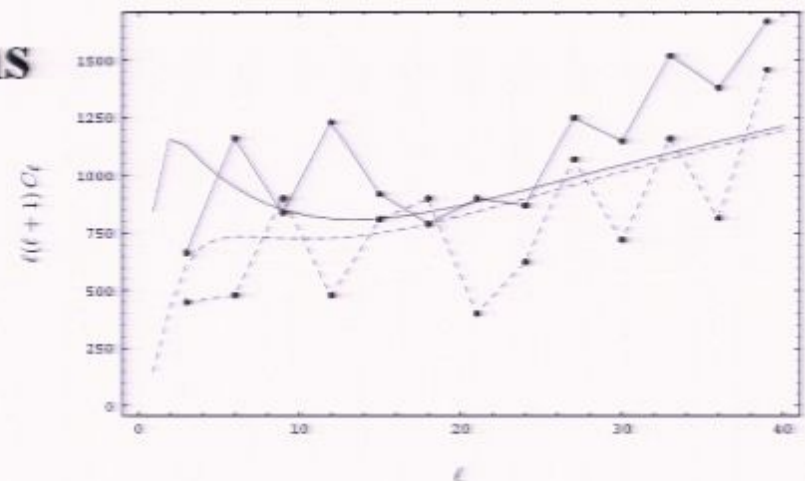
Advertisement: Limits on spatial variations from CMB

with Evan Donoghue

- Eriksen et al demonstrate potential asymmetry in CMB power spectrum
 - stable, $\sim 3\sigma$
 - occurs in low ℓ data – up to $\ell \sim 40$



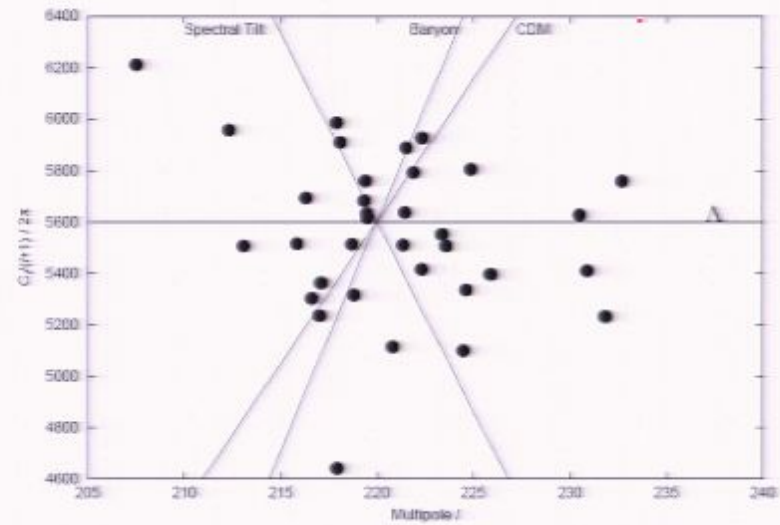
- Can this be due to spatial variations of some parameters?**
- especially cosmological constant?



Answer = NO

Reason: **First acoustic peak** shows no spatial asymmetry
- variation of any parameters would shift peak

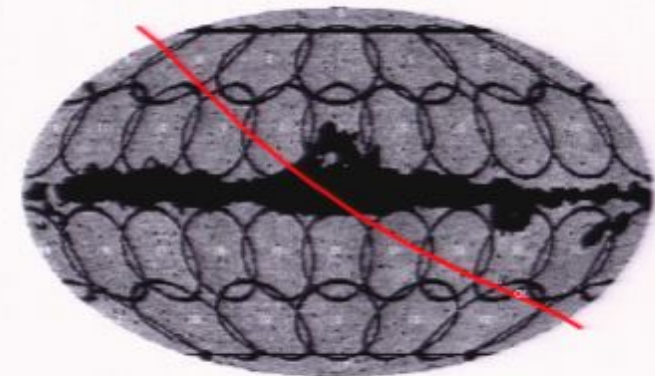
co-latitude	longitude	ℓ location	amplitude
0	0	223.3	5551
35	0	217.0	5235
35	60	215.8	5515
35	120	218.1	5909
35	180	207.5	6211
35	240	231.8	5231
35	300	232.7	5758
65	0	212.3	5957
65	36	217.9	4640
65	72	230.9	5410
65	108	224.5	5699
65	144	223.5	5506
65	180	221.5	5888
65	216	213.1	5506
65	252	217.9	5986
65	288	222.3	5927
65	324	224.6	5335
115	0	219.5	5633
115	36	222.3	5415
115	72	221.3	5510
115	108	219.5	5615
115	144	224.8	5804
115	180	216.3	5693
115	216	230.5	5627
115	252	220.8	5113
115	288	225.9	5395
115	324	219.4	5459
145	0	218.8	5315
145	60	219.3	5683
145	120	221.9	5792
145	180	216.6	5302
145	240	217.1	5362
145	300	221.4	5636
180	0	218.7	5513



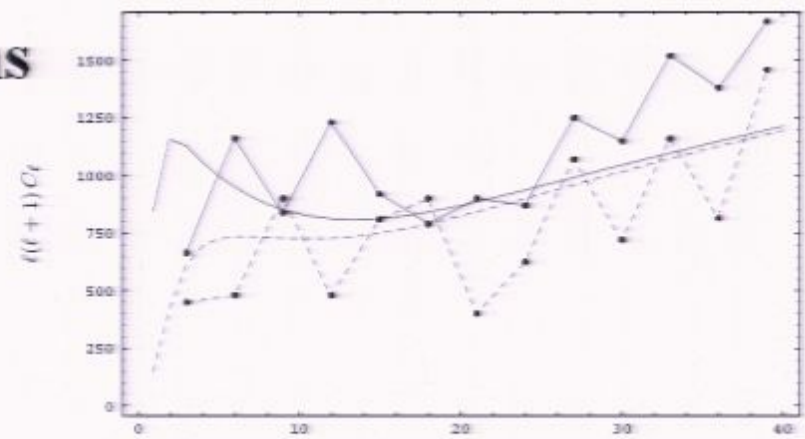
Advertisement: Limits on spatial variations from CMB

with Evan Donoghue

- Eriksen et al demonstrate potential asymmetry in CMB power spectrum
 - stable, $\sim 3\sigma$
 - occurs in low ℓ data – up to $\ell \sim 40$



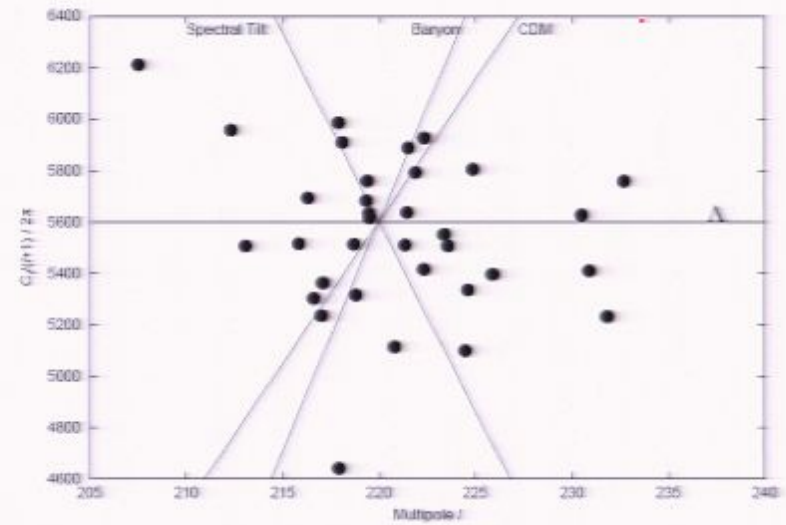
- Can this be due to spatial variations of some parameters?**
- especially cosmological constant?



Answer = NO

Reason: **First acoustic peak** shows no spatial asymmetry
- variation of any parameters would shift peak

co-latitude	longitude	ℓ location	amplitude
0	0	223.3	5551
35	0	217.0	5235
35	60	215.8	5515
35	120	218.1	5909
35	180	207.5	6211
35	240	231.8	5231
35	300	232.7	5758
65	0	212.3	5957
65	36	217.9	4640
65	72	230.9	5410
65	108	224.5	5099
65	144	223.5	5506
65	180	221.5	5888
65	216	213.1	5506
65	252	217.9	5986
65	288	222.3	5927
65	324	224.6	5335
115	0	219.5	5633
115	36	222.3	5415
115	72	221.3	5510
115	108	219.5	5615
115	144	224.8	5804
115	180	216.3	5693
115	216	230.5	5627
115	252	220.8	5113
115	288	225.9	5395
115	324	219.4	5459
145	0	218.8	5315
145	60	219.3	5683
145	120	221.9	5792
145	180	216.6	5302
145	240	217.1	5362
145	300	221.4	5636
180	0	218.7	5513



Result: Limits on spatial variation of Λ etc

lever arm $\sim 2 \times 13$ Gly

parameter	Baryon	<i>CDM</i>	Λ	amplitude	tilt
η fit	0.076 ± 0.048	0.004 ± 0.11	0.055 ± 0.035	0.027 ± 0.017	0.03 ± 0.02
2σ bound	0.17	0.28	0.125	0.061	0.057

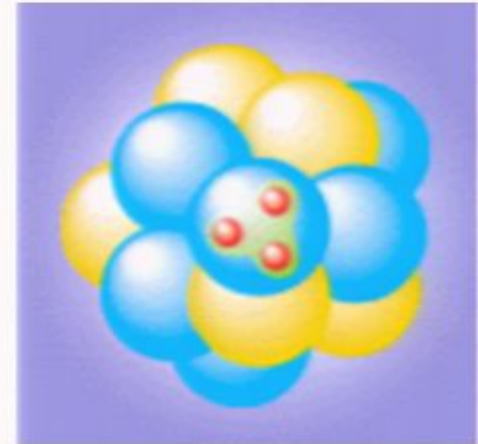
Table 3: Isotropy bounds when interpreted as variations of the underlying parameters. The first row of results gives the fit value of the fractional variation of each parameter, while the second row reports the 2σ upper limit on the possible variation.

Need to seek explanation elsewhere

- transient effect in inflation – kinetic energy or extra field

Nuclear binding

- a) EFT and contact interactions
- b) What is important?
- c) Dispersive representation
- d) Chiral treatment of low energy
- e) Finding the “sigma”



Result: Limits on spatial variation of Λ etc

lever arm $\sim 2 \times 13$ Gly

parameter	Baryon	<i>CDM</i>	Λ	amplitude	tilt
η fit	0.076 ± 0.048	0.004 ± 0.11	0.055 ± 0.035	0.027 ± 0.017	0.03 ± 0.02
2σ bound	0.17	0.28	0.125	0.061	0.057

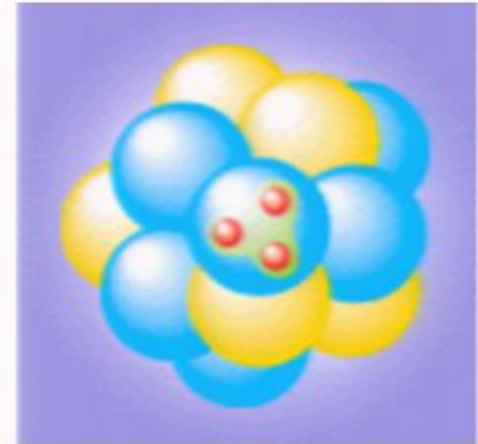
Table 3: Isotropy bounds when interpreted as variations of the underlying parameters. The first row of results gives the fit value of the fractional variation of each parameter, while the second row reports the 2σ upper limit on the possible variation.

Need to seek explanation elsewhere

- transient effect in inflation – kinetic energy or extra field

Nuclear binding

- a) EFT and contact interactions
- b) What is important?
- c) Dispersive representation
- d) Chiral treatment of low energy
- e) Finding the “sigma”



Traditionally described in terms of meson exchange

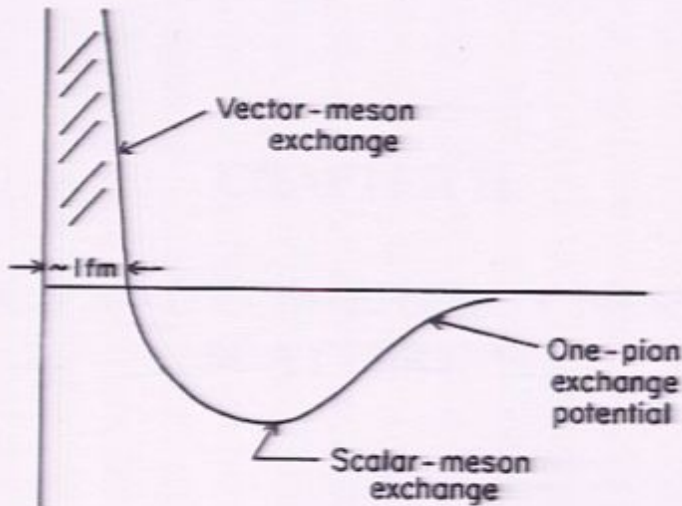


Fig. 2. Schematization of the nucleon-nucleon potential.

$$V(r) = \pm \frac{g^2}{4\pi} \frac{e^{-mr}}{r}$$

One pion exchange is not important for heavy nuclei
- key features are “sigma” and “omega” exchanges

I. Potentials → “contact” interactions

Nucleons are at very low energy ~ 10 MeV/nucleon

Effective field theory-

High energy effects (e.g. ρ, ω exchange) appear local at low energy

Example:

$$V(r) = -g_s^2 \frac{e^{-m_s r}}{4\pi r} \rightarrow -\frac{g_s^2}{m_s^2} \delta^3(r)$$

Then use contact interactions instead of potentials

- more general
- no assumptions about shape or origin

Serot
 Furnstahl
 -also Walech
 Madland
 Rusnak
 Hoch
 Entem
 Nilolas

Description of contact interactions

Nucleon densities:

$$\begin{aligned}
 \tilde{\rho}_s &\equiv \frac{\rho_s}{f_\pi^2 \Lambda} \equiv \frac{\bar{\psi} \psi}{f_\pi^2 \Lambda}, & \text{scalar} \\
 \tilde{\rho}_B &\equiv \frac{\rho_B}{f_\pi^2 \Lambda} \equiv \frac{\psi^\dagger \psi}{f_\pi^2 \Lambda}, & \text{vector} \\
 \tilde{\rho}_3 &\equiv \frac{\rho_3}{f_\pi^2 \Lambda} \equiv \frac{1}{2} \frac{\psi^\dagger \tau_3 \psi}{f_\pi^2 \Lambda}, \\
 \tilde{s}_i &\equiv \frac{s_i}{f_\pi^2 \Lambda} \equiv \frac{\bar{\psi} \sigma^{0i} \psi}{f_\pi^2 \Lambda}, \\
 \tilde{s}_{3i} &\equiv \frac{s_{3i}}{f_\pi^2 \Lambda} \equiv \frac{1}{2} \frac{\bar{\psi} \tau_3 \sigma^{0i} \psi}{f_\pi^2 \Lambda}
 \end{aligned}$$

Nuclear force described by contact interactions:

$$\begin{aligned}
 E = \int d^3x \sum_{\alpha}^{\text{occ}} \bar{\psi}_{\alpha} & (-i\beta \boldsymbol{\alpha} \cdot \boldsymbol{\nabla} + M) \psi_{\alpha} \\
 + f_\pi^2 \Lambda^2 \int d^3x \left\{ \tilde{\kappa}_2 \tilde{\rho}_s^2 - \tilde{\kappa}_d (\tilde{\nabla} \tilde{\rho}_s)^2 + \tilde{\kappa}_3 \tilde{\rho}_s^3 + \tilde{\kappa}_4 \tilde{\rho}_s^4 + \tilde{\eta}_1 \tilde{\rho}_B \tilde{\rho}_s + \tilde{\eta}_2 \tilde{\rho}_B^2 \tilde{\rho}_s^2 \right. \\
 \left. + \tilde{\zeta}_2 \tilde{\rho}_B^2 - \tilde{\zeta}_d (\tilde{\nabla} \tilde{\rho}_B)^2 + \tilde{\zeta}_4 \tilde{\rho}_B^4 - \tilde{\alpha}_1 \tilde{\rho}_s (\tilde{\nabla} \tilde{\rho}_s)^2 - \tilde{\alpha}_2 \tilde{\rho}_s (\tilde{\nabla} \tilde{\rho}_B)^2 \right. \\
 \left. + \text{isovector, tensor, and electromagnetic terms} \right. \\
 *** \quad \nearrow &
 \end{aligned}$$

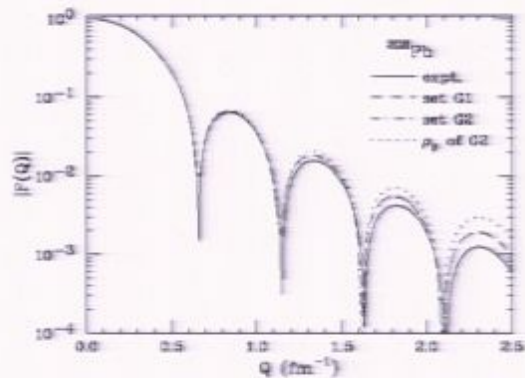
Some sample results:

TABLE II. Binding-energy systematics for sets G1, G2, and the point-coupling model of Ref. [71] (set PC). Binding energies per nucleon are given in MeV.

Set	^{16}O	^{40}Ca	^{48}Ca	^{88}Sr	^{208}Pb
G1	7.98	8.55	8.67	8.72	7.88
G2	7.97	8.55	8.68	8.72	7.87
PC	7.97	8.58	8.69	8.75	7.86
expt.	7.98	8.55	8.67	8.73	7.87

TABLE III. Rms charge radii (in fm) and d.m.s. radii (in fm) for sets G1, G2, and the point-coupling model of Ref. [71] (set PC).

Set	^{16}O		^{40}Ca		^{48}Ca		^{88}Sr		^{208}Pb	
	$\langle r^2 \rangle_{\text{ch}}^{\frac{1}{2}}$	R_{dms}								
G1	2.72	2.77	3.46	3.84	3.45	3.95	4.19	4.99	5.50	6.80
G2	2.73	2.77	3.46	3.84	3.45	3.95	4.19	5.00	5.50	6.80
PC	2.73		3.45		3.48		4.21		5.50	
expt.	2.74	2.76	3.45	3.85	3.45	3.96	4.20	4.99	5.50	6.78



Charge form factor of ^{208}Pb . The solid line is taken from experiment [77]. Form factors for the G1 and G2 parameter sets from Table I.

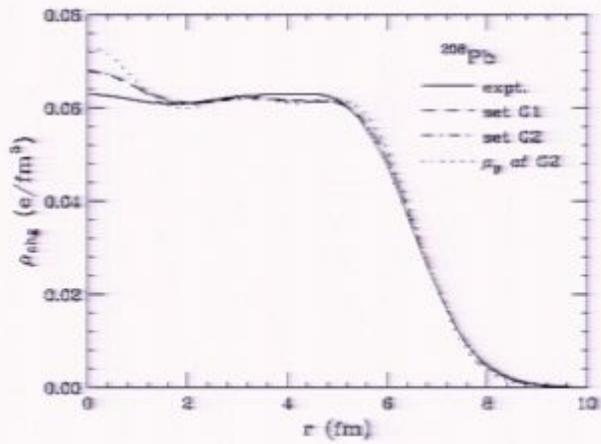


FIG. 7. Charge density of ^{208}Pb . The solid line is taken from experiment [77]. Charge densities are shown for the G1 and G2 parameter sets from Table I. Also shown is the point-proton density for set G2.

Serot
 Furnstahl
 -also Walech
 Madland
 Rusnak
 Hoch
 Entem
 Nilolas

Description of contact interactions

Nucleon densities:

$$\begin{aligned}
 \tilde{\rho}_s &\equiv \frac{\rho_s}{f_\pi^2 \Lambda} \equiv \frac{\bar{\psi} \psi}{f_\pi^2 \Lambda}, & \text{scalar} \\
 \tilde{\rho}_B &\equiv \frac{\rho_B}{f_\pi^2 \Lambda} \equiv \frac{\psi^\dagger \psi}{f_\pi^2 \Lambda}, & \text{vector} \\
 \tilde{\rho}_3 &\equiv \frac{\rho_3}{f_\pi^2 \Lambda} \equiv \frac{1}{2} \frac{\psi^\dagger \tau_3 \psi}{f_\pi^2 \Lambda}, \\
 \tilde{s}_i &\equiv \frac{s_i}{f_\pi^2 \Lambda} \equiv \frac{\bar{\psi} \sigma^{0i} \psi}{f_\pi^2 \Lambda}, \\
 \tilde{s}_{3i} &\equiv \frac{s_{3i}}{f_\pi^2 \Lambda} \equiv \frac{1}{2} \frac{\bar{\psi} \tau_3 \sigma^{0i} \psi}{f_\pi^2 \Lambda}
 \end{aligned}$$

Nuclear force described by contact interactions:

$$\begin{aligned}
 E = \int d^3x \sum_{\alpha}^{\text{occ}} \bar{\psi}_{\alpha} & (-i\beta \boldsymbol{\alpha} \cdot \boldsymbol{\nabla} + M) \psi_{\alpha} \\
 + f_\pi^2 \Lambda^2 \int d^3x \left\{ \tilde{\kappa}_2 \tilde{\rho}_s^2 - \tilde{\kappa}_d (\tilde{\nabla} \tilde{\rho}_s)^2 + \tilde{\kappa}_3 \tilde{\rho}_s^3 + \tilde{\kappa}_4 \tilde{\rho}_s^4 + \tilde{\eta}_1 \tilde{\rho}_B^2 \tilde{\rho}_s + \tilde{\eta}_2 \tilde{\rho}_B^2 \tilde{\rho}_s^2 \right. \\
 \left. + \tilde{\zeta}_2 \tilde{\rho}_B^2 - \tilde{\zeta}_d (\tilde{\nabla} \tilde{\rho}_B)^2 + \tilde{\zeta}_4 \tilde{\rho}_B^4 - \tilde{\alpha}_1 \tilde{\rho}_s (\tilde{\nabla} \tilde{\rho}_s)^2 - \tilde{\alpha}_2 \tilde{\rho}_s (\tilde{\nabla} \tilde{\rho}_B)^2 \right. \\
 \left. + \text{isovector, tensor, and electromagnetic terms} \right\}
 \end{aligned}$$

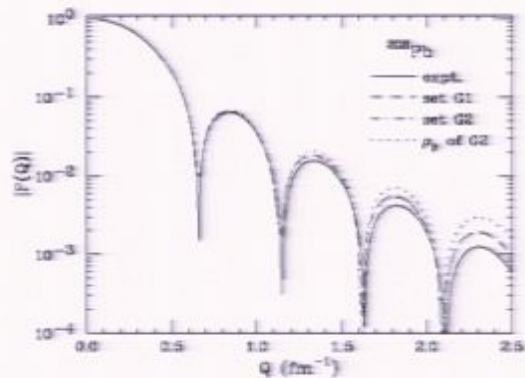
Some sample results:

TABLE II. Binding-energy systematics for sets G1, G2, and the point-coupling model of Ref. [71] (set PC). Binding energies per nucleon are given in MeV.

Set	^{16}O	^{40}Ca	^{48}Ca	^{88}Sr	^{208}Pb
G1	7.98	8.55	8.67	8.72	7.88
G2	7.97	8.55	8.68	8.72	7.87
PC	7.97	8.58	8.69	8.75	7.86
expt.	7.98	8.55	8.67	8.73	7.87

TABLE III. Rms charge radii (in fm) and d.m.s. radii (in fm) for sets G1, G2, and the point-coupling model of Ref. [71] (set PC).

Set	^{16}O		^{40}Ca		^{48}Ca		^{88}Sr		^{208}Pb	
	$\langle r^2 \rangle_{\text{ch}}^{\frac{1}{2}}$	R_{dms}								
G1	2.72	2.77	3.46	3.84	3.45	3.95	4.19	4.99	5.50	6.80
G2	2.73	2.77	3.46	3.84	3.45	3.95	4.19	5.00	5.50	6.80
PC	2.73		3.45		3.48		4.21		5.50	
expt.	2.74	2.76	3.45	3.85	3.45	3.96	4.20	4.99	5.50	6.78



Charge form factor of ^{208}Pb . The solid line is taken from experiment [77]. Form factors for the G1 and G2 parameter sets from Table I.

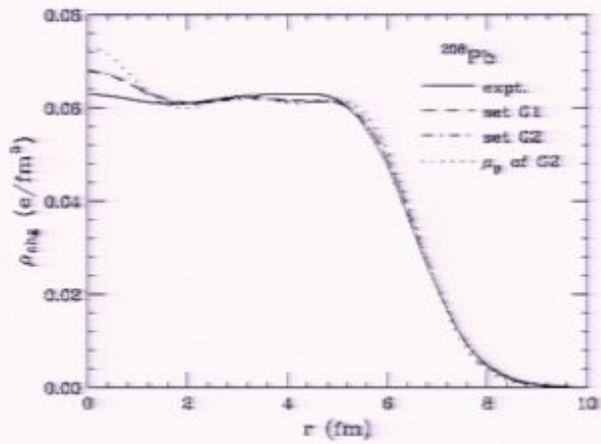


FIG. 7. Charge density of ^{208}Pb . The solid line is taken from experiment [77]. Charge densities are shown for the G1 and G2 parameter sets from Table I. Also shown is the point-proton density for set G2.

Only a small number of terms important:

Most contact terms have small effects

Most important are the “ σ, ω ” terms:

Scalar ~ 100 MeV
Vector $\sim +60$ MeV

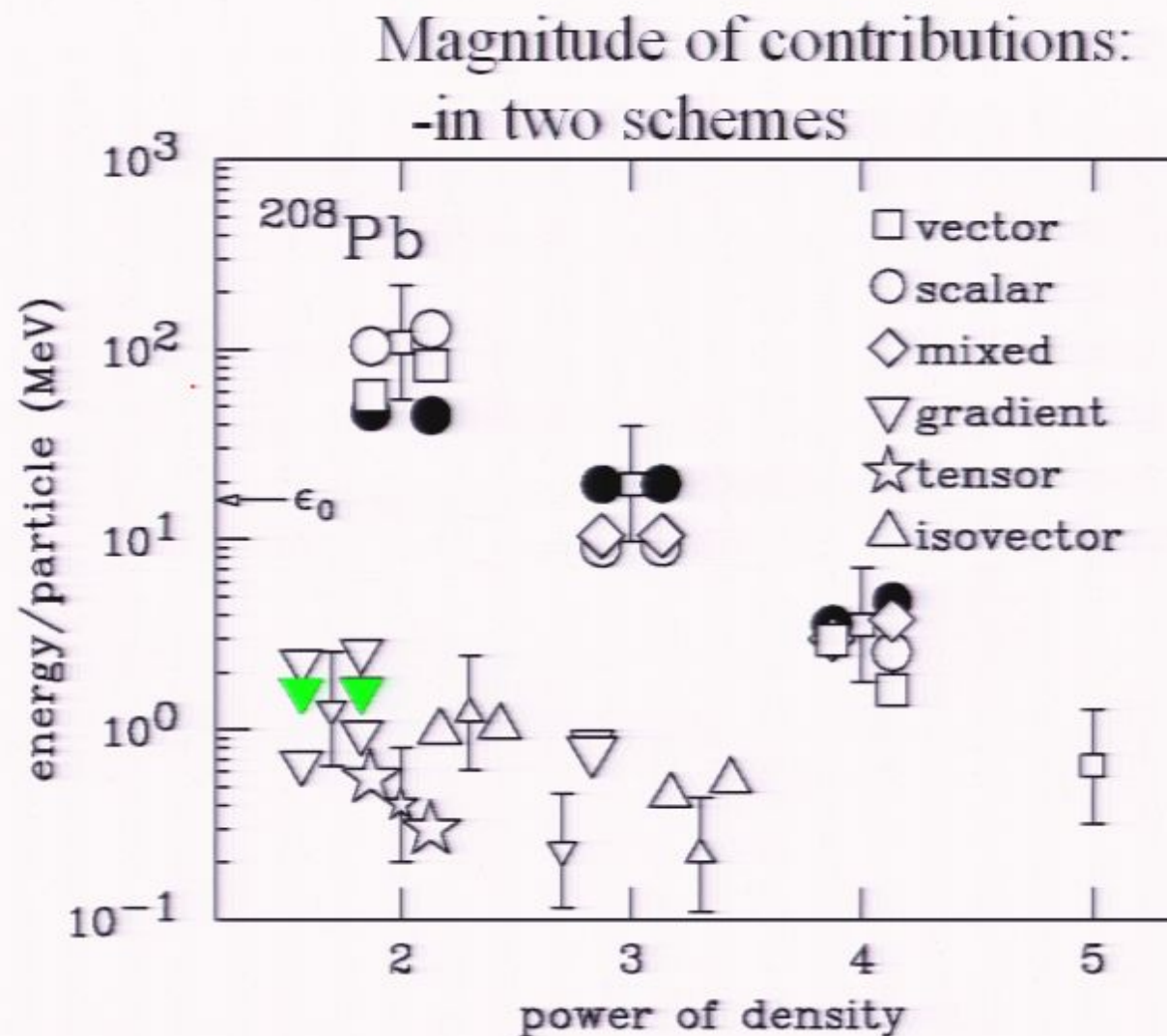


FIG. 2. Same as Fig. 1 for ^{208}Pb . Page 19/88

Serot
 Furnstahl
 -also Walech
 Madland
 Rusnak
 Hoch
 Entem
 Nilolas

Description of contact interactions

Nucleon densities:

$$\begin{aligned}
 \tilde{\rho}_s &\equiv \frac{\rho_s}{f_\pi^2 \Lambda} \equiv \frac{\bar{\psi} \psi}{f_\pi^2 \Lambda}, & \text{scalar} \\
 \tilde{\rho}_B &\equiv \frac{\rho_B}{f_\pi^2 \Lambda} \equiv \frac{\psi^\dagger \psi}{f_\pi^2 \Lambda}, & \text{vector} \\
 \tilde{\rho}_3 &\equiv \frac{\rho_3}{f_\pi^2 \Lambda} \equiv \frac{1}{2} \frac{\psi^\dagger \tau_3 \psi}{f_\pi^2 \Lambda}, \\
 \tilde{s}_i &\equiv \frac{s_i}{f_\pi^2 \Lambda} \equiv \frac{\bar{\psi} \sigma^{0i} \psi}{f_\pi^2 \Lambda}, \\
 \tilde{s}_{3i} &\equiv \frac{s_{3i}}{f_\pi^2 \Lambda} \equiv \frac{1}{2} \frac{\bar{\psi} \tau_3 \sigma^{0i} \psi}{f_\pi^2 \Lambda}
 \end{aligned}$$

Nuclear force described by contact interactions:

$$\begin{aligned}
 E = \int d^3x \sum_{\alpha}^{\text{occ}} \bar{\psi}_{\alpha} & (-i\beta \boldsymbol{\alpha} \cdot \boldsymbol{\nabla} + M) \psi_{\alpha} \\
 + f_\pi^2 \Lambda^2 \int d^3x \left\{ \tilde{\kappa}_2 \tilde{\rho}_s^2 - \tilde{\kappa}_d (\tilde{\nabla} \tilde{\rho}_s)^2 + \tilde{\kappa}_3 \tilde{\rho}_s^3 + \tilde{\kappa}_4 \tilde{\rho}_s^4 + \tilde{\eta}_1 \tilde{\rho}_B \tilde{\rho}_s + \tilde{\eta}_2 \tilde{\rho}_B^2 \tilde{\rho}_s^2 \right. \\
 \left. + \tilde{\zeta}_2 \tilde{\rho}_B^2 - \tilde{\zeta}_d (\tilde{\nabla} \tilde{\rho}_B)^2 + \tilde{\zeta}_4 \tilde{\rho}_B^4 - \tilde{\alpha}_1 \tilde{\rho}_s (\tilde{\nabla} \tilde{\rho}_s)^2 - \tilde{\alpha}_2 \tilde{\rho}_s (\tilde{\nabla} \tilde{\rho}_B)^2 \right. \\
 \left. + \text{isovector, tensor, and electromagnetic terms} \right\}
 \end{aligned}$$

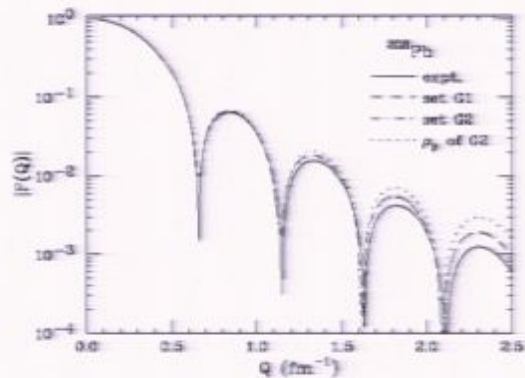
Some sample results:

TABLE II. Binding-energy systematics for sets G1, G2, and the point-coupling model of Ref. [71] (set PC). Binding energies per nucleon are given in MeV.

Set	^{16}O	^{40}Ca	^{48}Ca	^{88}Sr	^{208}Pb
G1	7.98	8.55	8.67	8.72	7.88
G2	7.97	8.55	8.68	8.72	7.87
PC	7.97	8.58	8.69	8.75	7.86
expt.	7.98	8.55	8.67	8.73	7.87

TABLE III. Rms charge radii (in fm) and d.m.s. radii (in fm) for sets G1, G2, and the point-coupling model of Ref. [71] (set PC).

Set	^{16}O		^{40}Ca		^{48}Ca		^{88}Sr		^{208}Pb	
	$\langle r^2 \rangle_{\text{ch}}^{\frac{1}{2}}$	R_{dms}								
G1	2.72	2.77	3.46	3.84	3.45	3.95	4.19	4.99	5.50	6.80
G2	2.73	2.77	3.46	3.84	3.45	3.95	4.19	5.00	5.50	6.80
PC	2.73	3.45		3.48		4.21		5.50		
expt.	2.74	2.76	3.45	3.85	3.45	3.96	4.20	4.99	5.50	6.78



Charge form factor of ^{208}Pb . The solid line is taken from experiment [77]. Form factors for the G1 and G2 parameter sets from Table I.

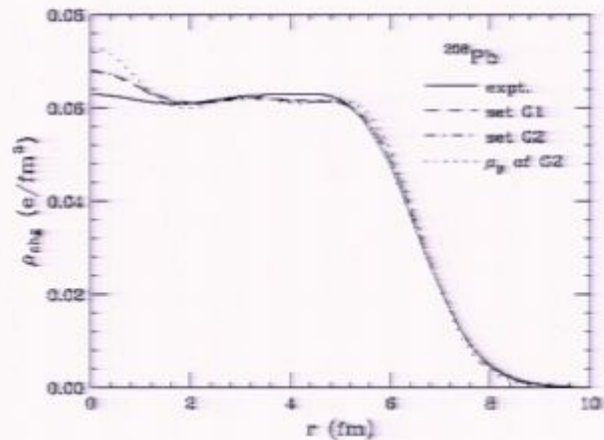


FIG. 7. Charge density of ^{208}Pb . The solid line is taken from experiment [77]. Charge densities are shown for the G1 and G2 parameter sets from Table I. Also shown is the point-proton density for set G2.

Only a small number of terms important:

Most contact terms have small effects

Most important are the “ σ, ω ” terms:

Scalar ~ 100 MeV
Vector $\sim +60$ MeV

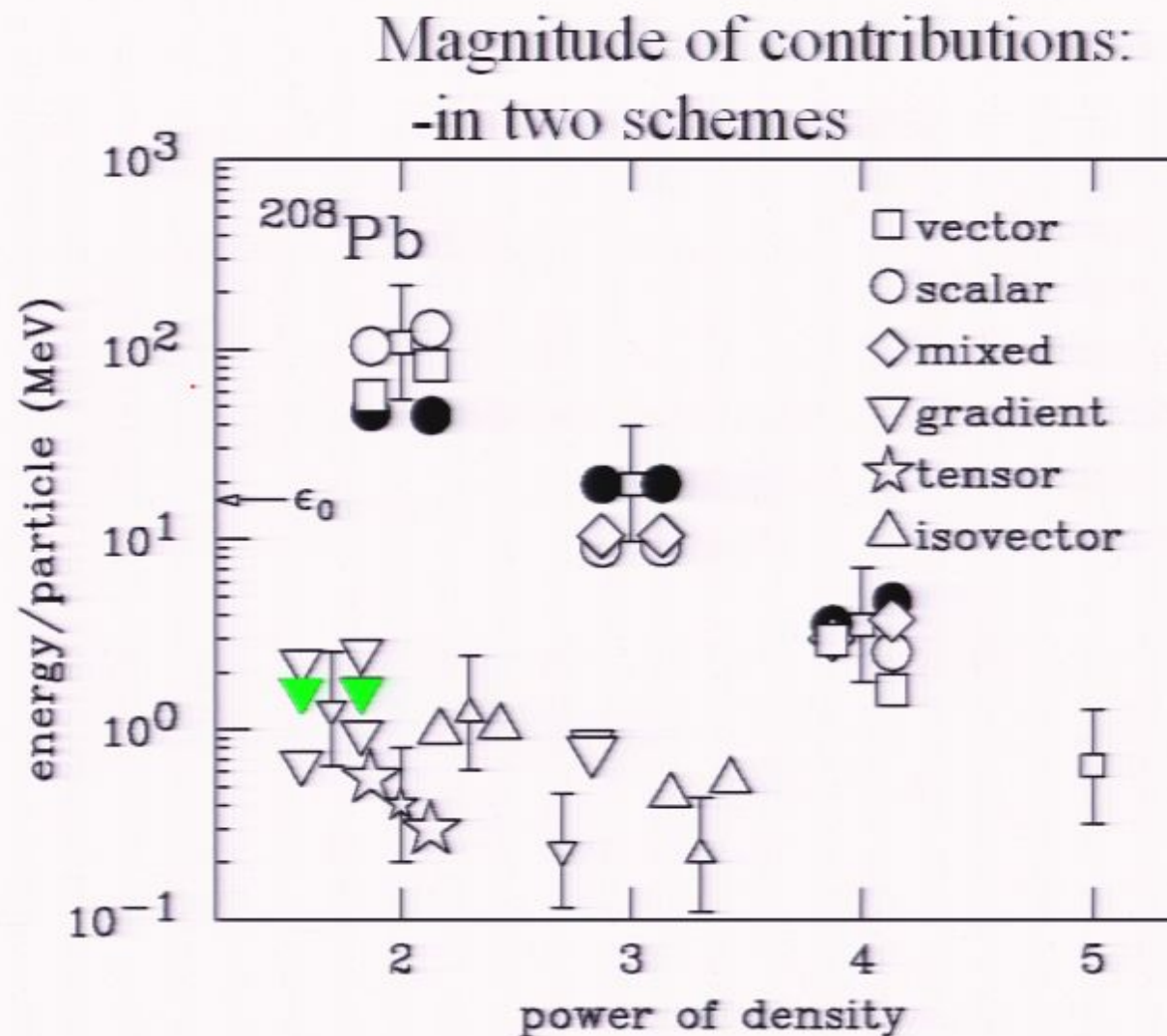


FIG. 2. Same as Fig. 1 for ^{208}Pb . Page 22/88

Results to be extracted:

Two main interactions: -both ρ^2

Attractive scalar contact term

Repulsive vector contact term

$$H = G_S (\bar{N}N)(\bar{N}N) + G_V (\bar{N}\gamma^\mu N)(\bar{N}\gamma_\mu N)$$

Known contributions from each

-of order 100 MeV/nucleon

Significant cancellation occurs

Primary effects in nuclear binding

- know the main contributions to binding energy

$$\eta_v = \frac{G_V}{G_V^{\text{physical}}}$$

Let:

$$\eta_s = \frac{G_S}{G_S^{\text{physical}}}$$

Then for ^{208}Pb :

$$\frac{\text{B.E.}}{A} \sim -104\eta_s + 57\eta_v + 18 + \text{K.E}$$

or in general: $\frac{\text{B.E.}}{A} = -(120 - \frac{97}{A^{1/3}})\eta_s + (67 - \frac{57}{A^{1/3}})\eta_v + \text{residual terms}$

Constructing the contact interactions

Recall:

$\delta^3(\mathbf{r})$ is Fourier transform of a constant

$V(q=0)$ gives the coefficient of the contact potential
 $-q^2$ dependence gives the gradient expansion

$$H = G_S (\bar{N} N) (\bar{N} N) + G_V (\bar{N} \gamma^\mu N) (\bar{N} \gamma_\mu N)$$

Consider the scattering amplitude in different channels

$$M_s(q^2) = G_s + H_s q^2 + \dots$$

Rigorous “old” technology -dispersion relations

Cottingham
Vinh Mau

NN → NN amplitude satisfies t-channel dispersion relation

- cross reaction to $N\bar{N} \rightarrow N\bar{N}$

- decompose in partial waves

- write dispersion relation

- first cuts in isoscalar S,P waves at $4 m_\pi^2, 9 m_\pi^2$

$$M(s, t) = \frac{1}{\pi} \int_{4m_\pi^2}^{\infty} d\mu^2 \frac{ImM(s, \mu^2)}{\mu^2 - t - i\epsilon}$$

Take limit of low energy ($s \rightarrow 4 m_N^2$) to define potential in each channel and use:

$$\rho_S(\mu) = ImV_S(q = i\mu)$$

Using dispersive representation:

Momentum space potential:

$$V_S(q^2) = \frac{2}{\pi} \int_{2m_\pi}^{\infty} d\mu \ \mu \frac{\rho_S(\mu)}{\mu^2 + q^2}$$

Contact interaction:

$$G_{S,V} = \frac{2}{\pi} \int_{(2m_\pi, 3m_\pi)}^{\infty} \frac{d\mu}{\mu} \ \rho_{S,V}(\mu^2)$$

For orientation: sigma potential from $\rho(\mu) = -\pi g_\sigma^2 \delta(\mu^2 - m_\sigma^2)$

Rigorous “old” technology -dispersion relations

Cottingham
Vinh Mau

NN → NN amplitude satisfies t-channel dispersion relation

- cross reaction to $N\bar{N} \rightarrow N\bar{N}$

- decompose in partial waves

- write dispersion relation

- first cuts in isoscalar S,P waves at $4 m_\pi^2, 9 m_\pi^2$

$$M(s, t) = \frac{1}{\pi} \int_{4m_\pi^2}^{\infty} d\mu^2 \frac{ImM(s, \mu^2)}{\mu^2 - t - i\epsilon}$$

Take limit of low energy ($s \rightarrow 4 m_N^2$) to define potential in each channel and use:

$$\rho_S(\mu) = ImV_S(q = i\mu)$$

Using dispersive representation:

Momentum space potential:

$$V_S(q^2) = \frac{2}{\pi} \int_{2m_\pi}^{\infty} d\mu \ \mu \frac{\rho_S(\mu)}{\mu^2 + q^2}$$

Contact interaction:

$$G_{S,V} = \frac{2}{\pi} \int_{(2m_\pi, 3m_\pi)}^{\infty} \frac{d\mu}{\mu} \ \rho_{S,V}(\mu^2)$$

For orientation: sigma potential from $\rho(\mu) = -\pi g_\sigma^2 \delta(\mu^2 - m_\sigma^2)$

The experimental information on I=0, S=0 channel

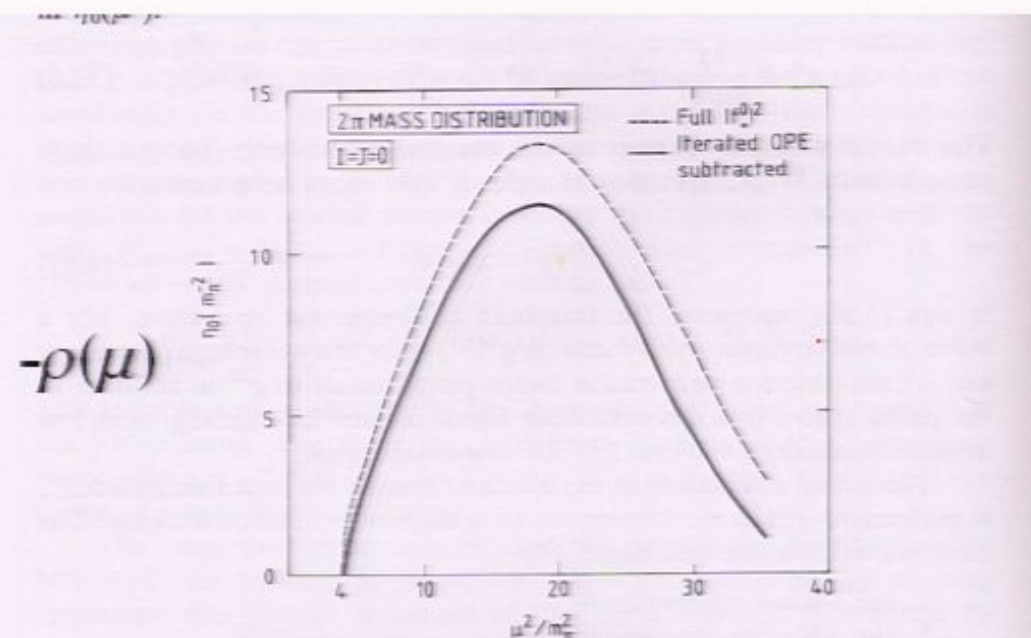


FIG. 3.15. The 2π mass distribution $\eta_0(\mu^2)$ in the 2π -exchange potential for the case of $I_{\pi\pi} = J_{\pi\pi} = 0$ exchange.^[5]

from
“Paris
potential”

fits to scatterin
data

This is the “sigma”

We can calculate this in Chiral Perturbation Theory

We have had reasonable success calculating pionic processes

Sample: $\gamma\gamma \rightarrow \pi^0 \pi^0$

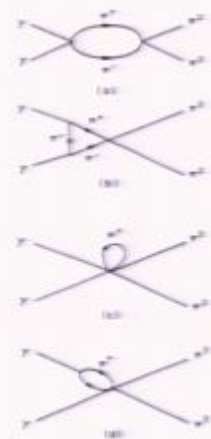
General structure:

- photons couple to charged pions
- charged pions rescatter to neutral pions
- rescattering determined by $\pi\pi$ scattering phases

$$Amp(\gamma\gamma \rightarrow \pi\pi) = P(\mu)\Omega(\mu)$$

$$\Omega(\mu) = \exp\left[\frac{\mu^2}{\pi} \int \frac{ds}{s} \frac{\delta(s)}{s - \mu^2}\right]$$

Omnes function



$$\gamma\gamma \rightarrow \pi^0 \pi^0$$

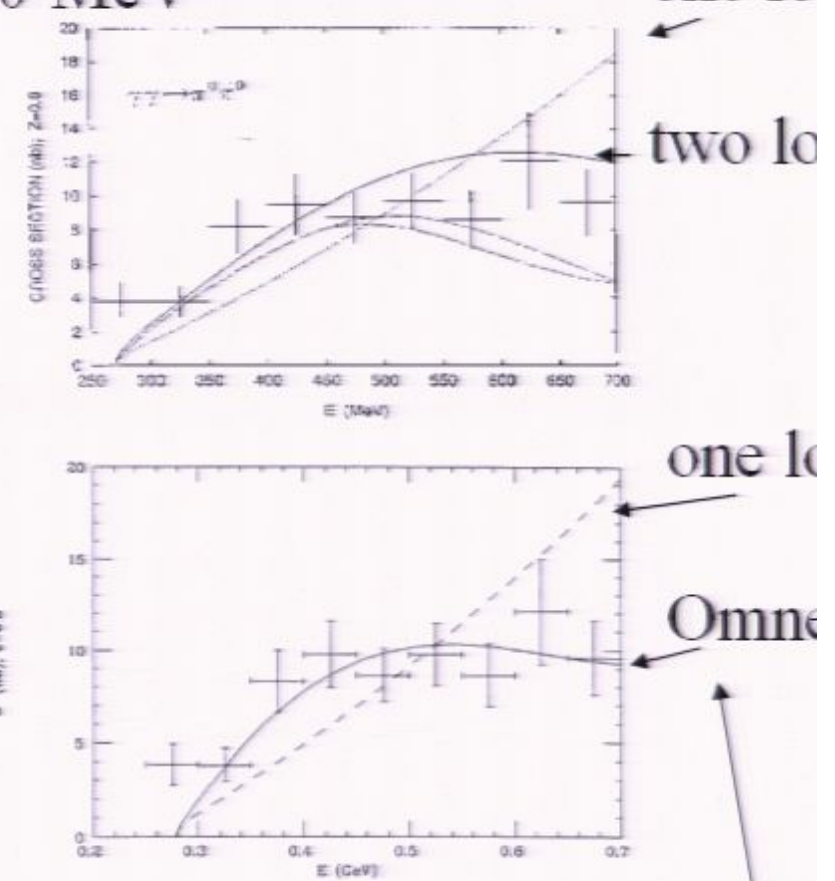
JFD and Holstein

Starts at one loop

- finite – no free parameters
- result grows with energy
- violates unitarity bound around 600 MeV

Onnes solution

- respects unitarity bound
- agrees with data
- also closely matches 2 loop result



This is the analogue of the nuclear calculation to follow

Interactions of pions with nucleons:

$$\pi \gamma \rightarrow \bullet = \frac{g_A}{F_\pi} \gamma_\mu \gamma_5$$

$$\gamma \rightarrow \bullet = \frac{1}{F_\pi^2} [2c_1 m_\pi^2 + c_2 E_1 E_2 + c_3 q_1 \cdot q_2]$$

- c_1, c_3 are known low energy constants from $NN\pi\pi$ interactions

$$c_1 = -(0.5 \rightarrow 0.9) \text{ GeV}^{-1},$$

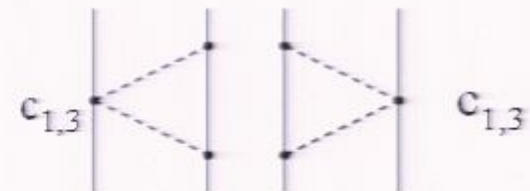
$$c_2 = 3.3 \pm 0.2$$

$$c_3 = -(3.9 \rightarrow 5.3) \text{ GeV}^{-1}$$

Chiral calculation via spectral function:

Epelbaum, Glöckle, Meissner
Kaiser Brockmann, Weise

Leading chiral loop – called NNLO



$$\rho_S^{\text{NNLO}}(\mu) = \frac{3g_A^2}{64F_\pi^4} \left[4c_1 m_\pi^2 + c_3 (\mu^2 - 2m_\pi^2) \right] \frac{(\mu^2 - 2m_\pi^2)}{\mu} \theta(\mu - 2m_\pi)$$

Also next contribution: “NNNLO”

Kaiser



$$\begin{aligned} \rho_S^{\text{NNNLO}}(\mu) &= -\frac{3}{32\pi F_\pi^4} \sqrt{1 - \frac{4m_\pi^2}{\mu^2}} \theta(\mu - 2m_\pi) \\ &\quad \left(\left[4c_1 m_\pi^2 + \frac{c_2}{6} (\mu^2 - 4m_\pi^2) + c_3 (\mu^2 - 2m_\pi^2) \right]^2 + \frac{c_2^2}{45} (\mu^2 - 4m_\pi^2)^2 \right) \end{aligned} \quad (38)$$

Including rescattering:

Gasser JFD Leutwyler

- elastic rescattering
- single channel problem

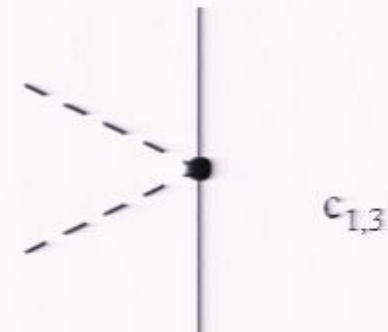
reaction $N\bar{N} \rightarrow \pi\pi$ at $2m_\pi < E < 1\text{GeV}$

rescattering only in elastic channel $\pi\pi \rightarrow \pi\pi$

Solution:

$$\mathcal{M}(N\bar{N} \rightarrow \pi\pi) = P(\mu)\Omega(\mu)$$

$$\Omega(\mu) = \exp\left[\frac{\mu^2}{\pi} \int \frac{ds}{s} \frac{\delta(s)}{s - \mu^2}\right] \quad \text{Omnes function}$$



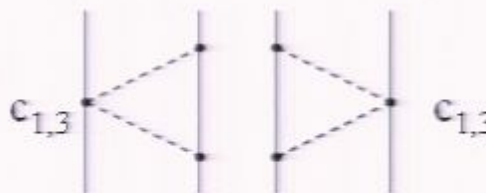
Approximation method:

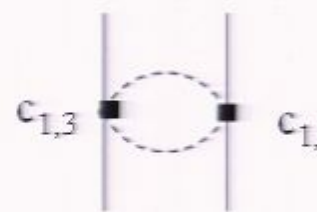
Match chiral prediction to Omnes solution order by order
Experience – this provides extrapolation to higher energy

Matching to the chiral calculations:

Full result must agree with chiral calculation at low energy
-NN $\pi\pi$ vertex determined by $c_{1,3}$

Modify ImV(μ) calculations:

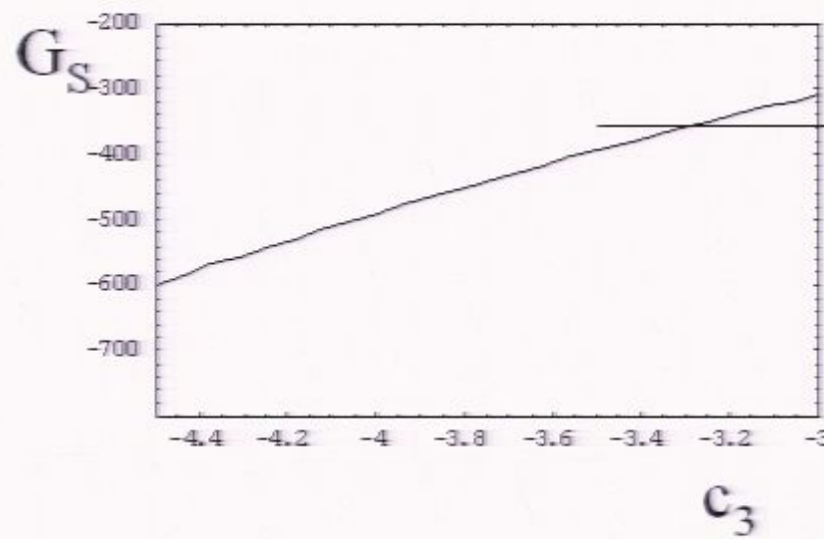
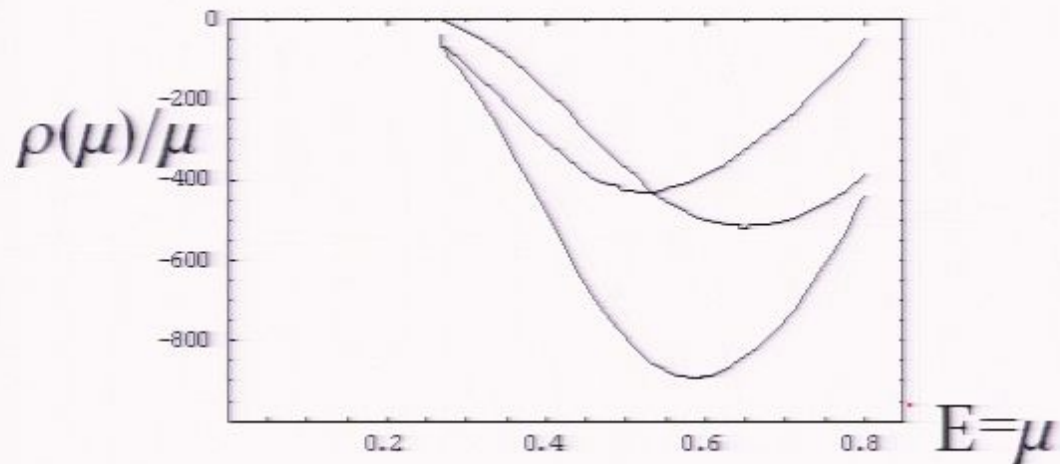
NNLO  $\Omega(\mu) + \Omega^\dagger(\mu)$

“NNNLO”  $|\Omega(\mu)|^2$

Result:

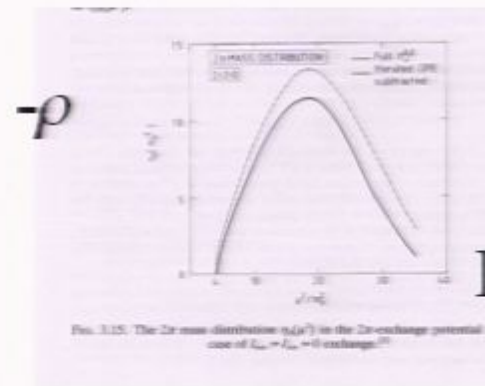
$$\rho_S(\mu) = \rho_S^{NNLO} \operatorname{Re}\Omega(\mu) + \rho_S^{NNNLO} |\Omega(\mu)|^2$$

Results:



favored value

Recall:



Easily reproduces correct shape and strength!

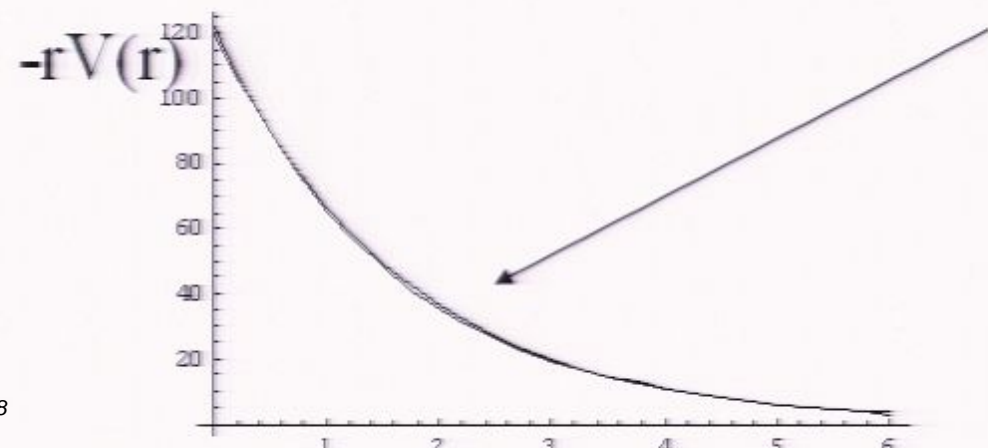
Reproduces “ σ potential” very closely

Recall momentum space dispersion relation:

$$V_S(q^2) = \frac{2}{\pi} \int_{2m_\pi}^{\infty} d\mu \ \mu \frac{\rho_S(\mu)}{\mu^2 + q^2}$$

Define coordinate space potential by F.T.

$$V_S(r) = \frac{1}{2\pi^2 r} \int_{2m_\pi}^{\infty} d\mu \ \mu e^{-\mu r} \rho_S(\mu)$$



Sigma potential

$$V(r) = \pm \frac{g^2}{4\pi} \frac{e^{-mr}}{r}$$

vs ChPTh $\rho(\mu)$

The modern story of the sigma:

Consequence of Goldstone dynamics

Caprini,
Colangelo
Leutwyler

ChPT describes $\pi\pi$ scattering using only F_π, m_π

- analytic continuation reveals pole far from real axis

$$M_\sigma = 441 {}^{+16}_{-8} \text{ MeV}, \quad \Gamma_\sigma = 544 {}^{+18}_{-25} \text{ MeV}$$

- would appear in **any** chiral theory
- sigma does not drive $\pi\pi$ scattering, it is secondary effect

In nuclei:

- similar result – fundamental sigma is not driving feature
- chiral dynamics control the spectral function
- uses $\pi\pi$ phase shifts, so sigma is “present” far from real axis
- but key features are couplings of pions and the pion mass

Overall: More understandable picture

Only a few numbers are important

- contact interactions
- effective field theory treatment

Contact interactions have simple ingredients

- dispersive representation

“Sigma” channel is calculable with reasonable control

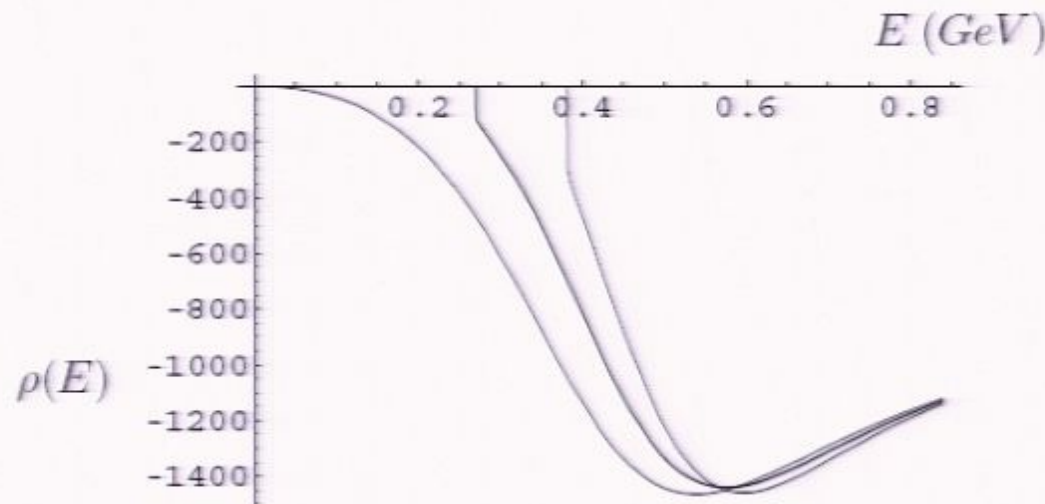
- no need to postulate a resonance at 600 MeV
- strength is reasonable

Application: m_q dependence of binding

Reasonable control over the ingredients to this calculation:

Main difference is kinematic

-in region where we trust calculation

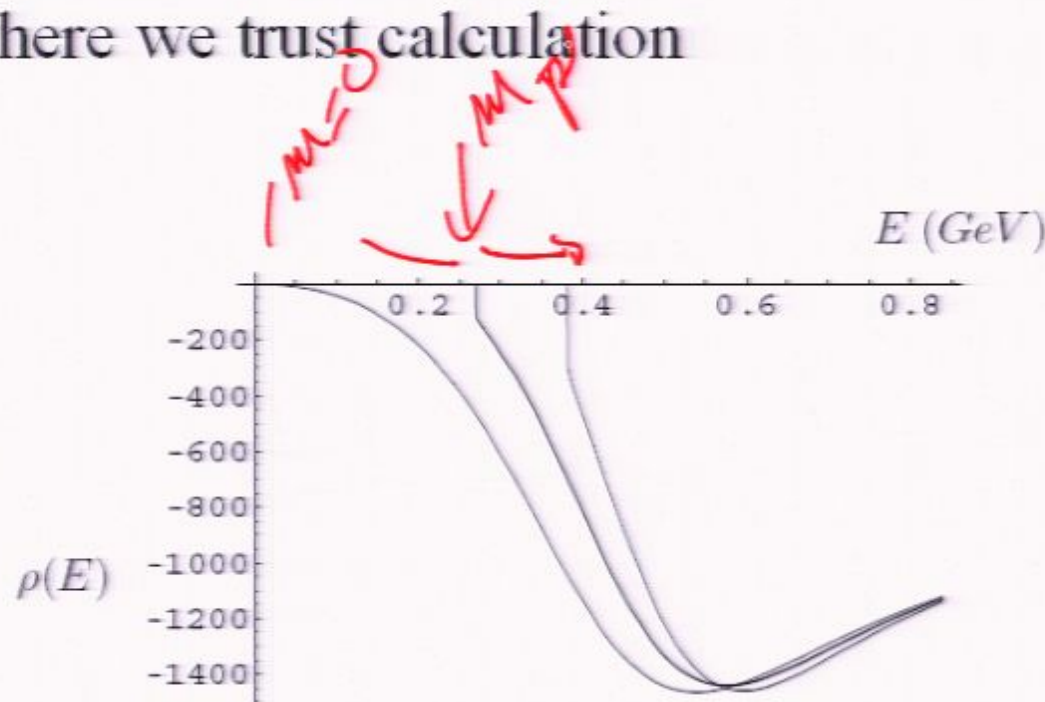


Application: m_q dependence of binding

Reasonable control over the ingredients to this calculation:

Main difference is kinematic

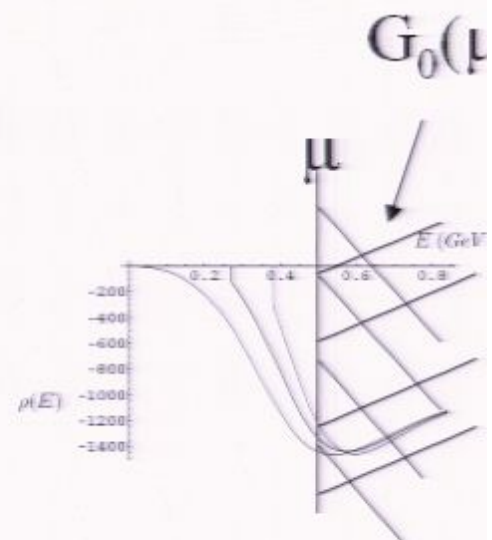
-in region where we trust calculation



Two possible pathways:

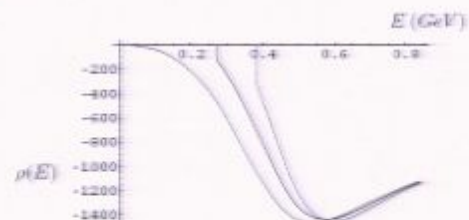
1) “Pure” ChPTh

- treat low energy region with chiral methods
 - find **enhanced** sensitivity
- use local constant for high energy region
 - assume normal sensitivity m_π^2/Λ^2



2) Full treatment through “sigma” region

- include effects up to 0.85 GeV
- include all known mass effects



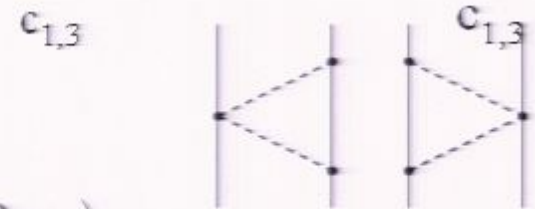
Essentially identical results

Spectral functions depend on quark masses:

Epelbaum, Glöckle, Meissn
Kaiser Brockmann, Weise

NNLO

$$\rho_S^{\text{NNLO}}(\mu) = \frac{3g_A^2}{64F_\pi^4} \left[4c_1 m_\pi^2 + c_3(\mu^2 - 2m_\pi^2) \right] \frac{(\mu^2 - 2m_\pi^2)}{\mu} \theta(\mu - 2m_\pi)$$



“NNNLO”

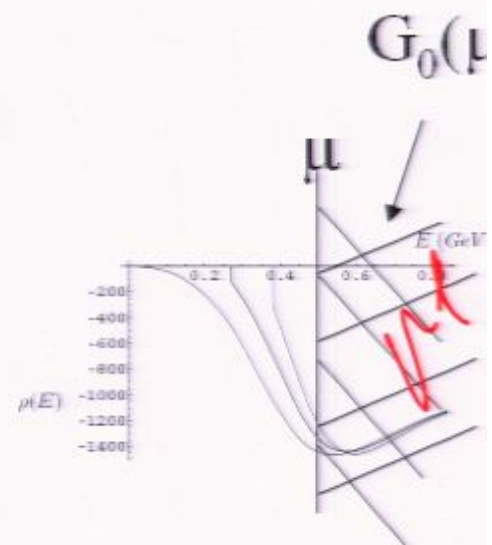
$$\begin{aligned} \rho_S^{\text{NNNLO}}(\mu) &= -\frac{3}{32\pi F_\pi^4} \sqrt{1 - \frac{4m_\pi^2}{\mu^2}} \theta(\mu - 2m_\pi) \\ &\quad \left(\left[4c_1 m_\pi^2 + \frac{c_2}{6}(\mu^2 - 4m_\pi^2) + c_3(\mu^2 - 2m_\pi^2) \right]^2 + \frac{c_2^2}{45}(\mu^2 - 4m_\pi^2)^2 \right) \end{aligned} \quad (38)$$



Two possible pathways:

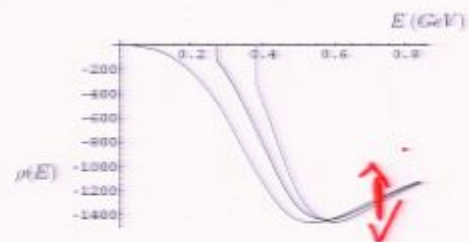
1) “Pure” ChPTh

- treat low energy region with chiral methods
 - find **enhanced** sensitivity
- use local constant for high energy region
 - assume normal sensitivity m_π^2/Λ^2



2) Full treatment through “sigma” region

- include effects up to 0.85 GeV
- include all known mass effects



Essentially identical results

$$m_T^2 = m_g B_0$$

D405

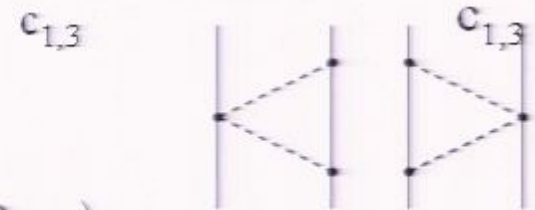
347

Spectral functions depend on quark masses:

Epelbaum, Glöckle, Meissn
Kaiser Brockmann, Weise

NNLO

$$\rho_S^{\text{NNLO}}(\mu) = \frac{3g_A^2}{64F_\pi^4} \left[4c_1 m_\pi^2 + c_3(\mu^2 - 2m_\pi^2) \right] \frac{(\mu^2 - 2m_\pi^2)}{\mu} \theta(\mu - 2m_\pi)$$



“NNNLO”

$$\begin{aligned} \rho_S^{\text{NNNLO}}(\mu) &= -\frac{3}{32\pi F_\pi^4} \sqrt{1 - \frac{4m_\pi^2}{\mu^2}} \theta(\mu - 2m_\pi) \\ &\quad \left(\left[4c_1 m_\pi^2 + \frac{c_2}{6}(\mu^2 - 4m_\pi^2) + c_3(\mu^2 - 2m_\pi^2) \right]^2 + \frac{c_2^2}{45}(\mu^2 - 4m_\pi^2)^2 \right) \end{aligned} \quad (38)$$

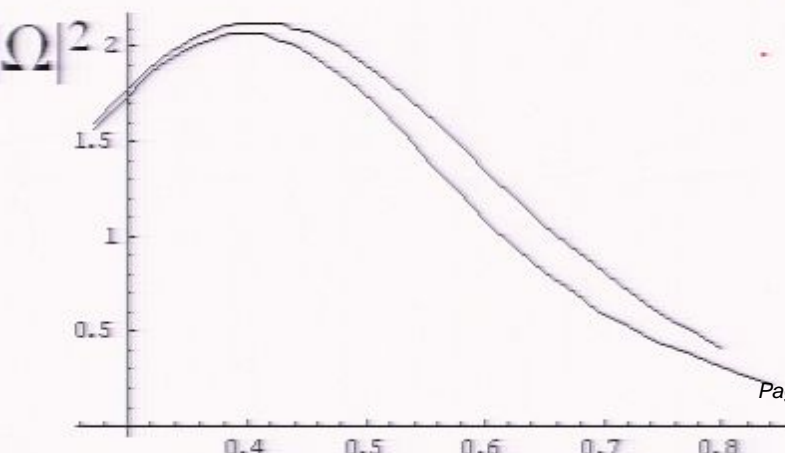
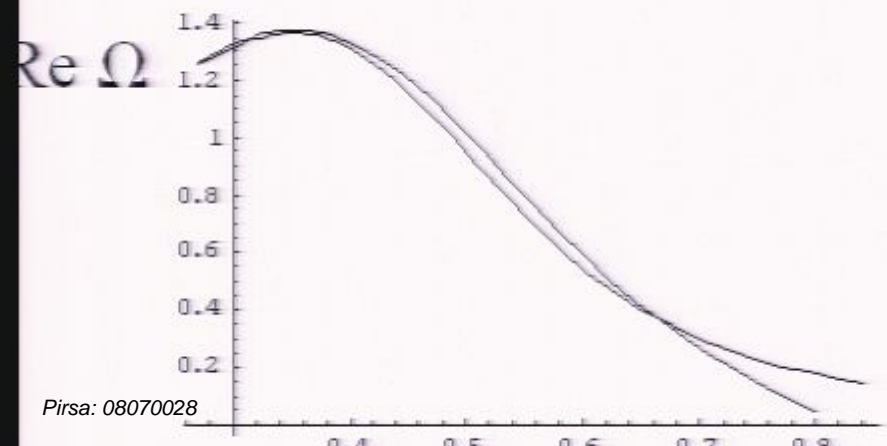
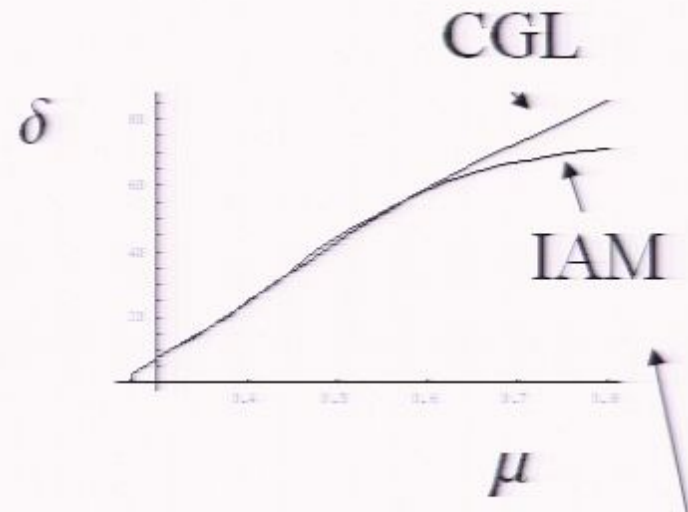


Pion scattering

In order to vary mass, I use “inverse amplitude method” for scattering information

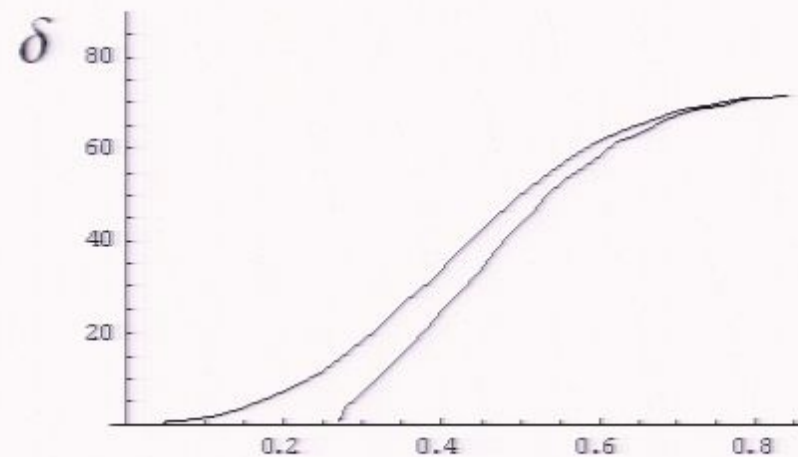
$$T_{00} = t_2 + t_4 + \dots \rightarrow \frac{t_2^2}{t_2 - t_4}$$

exactly satisfies unitarity
reasonable representation of CGL results

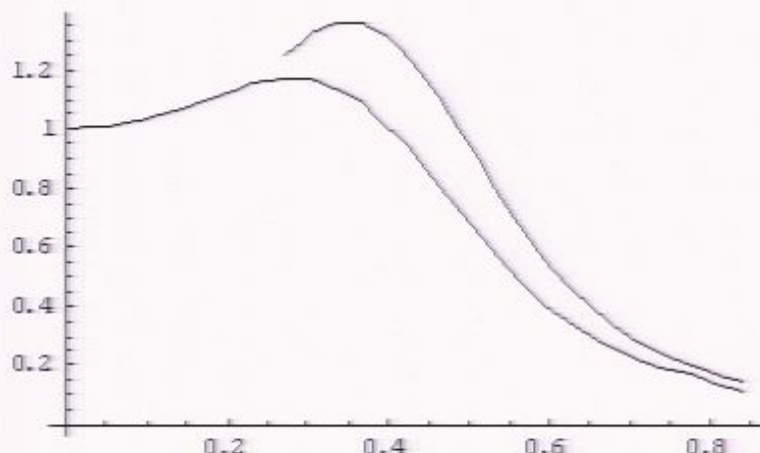


Omnès function – physical vs chiral limit

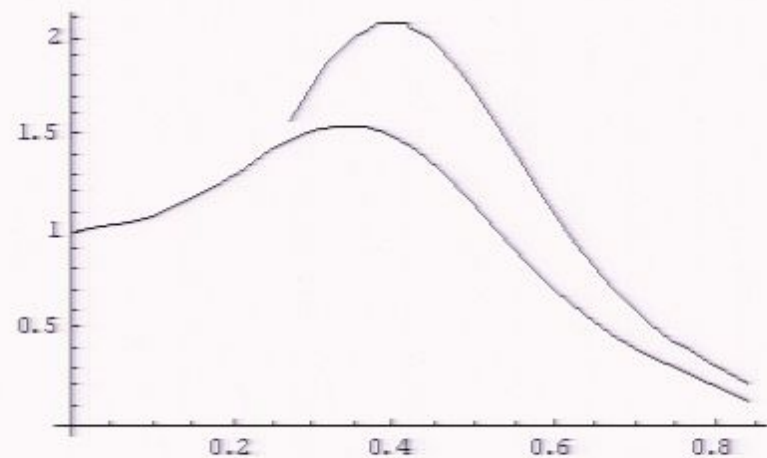
Phase shift



$\text{Re } \Omega$



$|\Omega|^2$



Dependence of pion coupling on quark mass

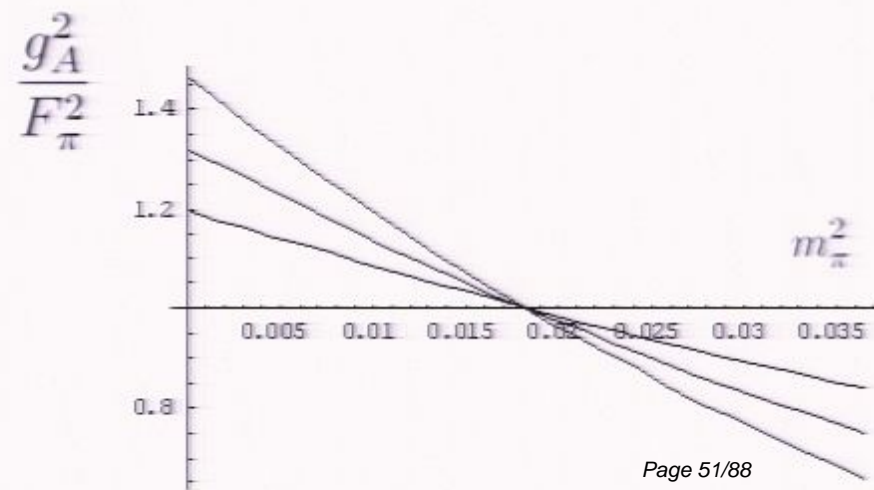
Pion coupling is g_A/F_π , with known behavior

$$F_\pi = F_0 \left[1 - \frac{1}{16\pi^2 F_0^2} m_\pi^2 \left(\ln \frac{m_\pi^2}{m_{ph}^2} + \bar{l}_4 \right) \right]$$
$$g_A = g_0 \left[1 - \frac{2g_0^2 + 1}{16\pi^2 F_0^2} m_\pi^2 \ln \frac{m_\pi^2}{m_{ph}^2} - \frac{g_0^2 m_\pi^2}{16\pi^2 F_0^2} + \frac{4m_\pi^2 \bar{d}_{16}}{g_0} \right]$$

many references

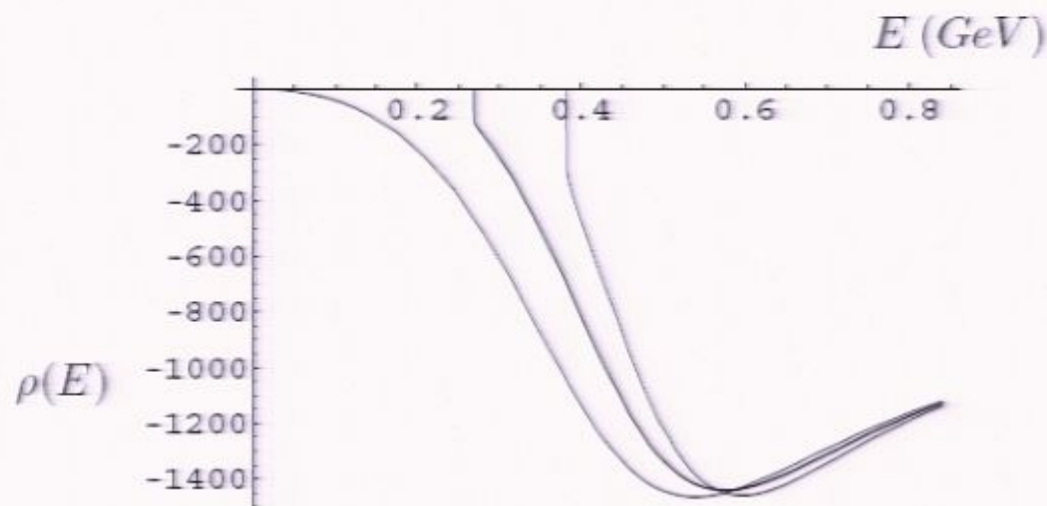
with $\bar{l}_4 = 4.4 \pm 0.2$ and $\bar{d}_{16} = -1.0 \pm 0.7$

Uncertainty of d_{16}
is largest uncertainty



Result is mostly related to kinematic threshold

Threshold region is highly reliable:



Numerical results ($c_3 = -3.6$) :

Chiral limit: $G_S = -427 \pm 26$

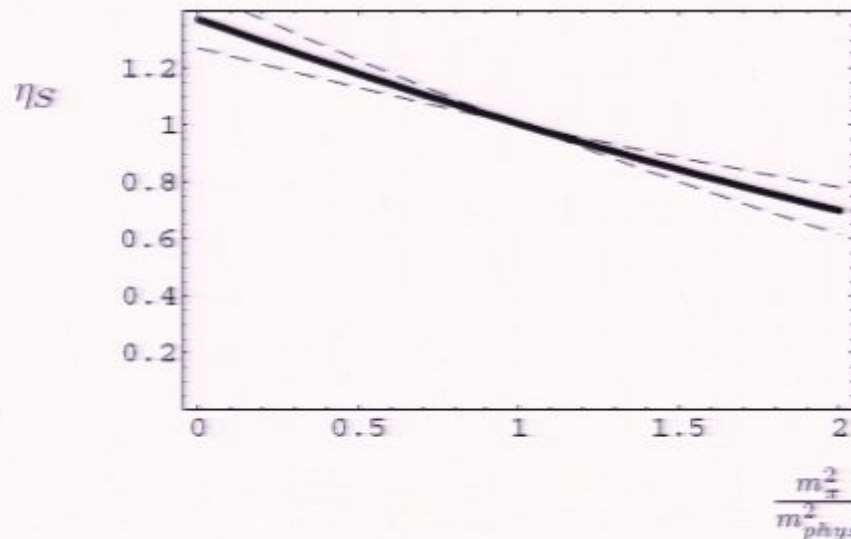
12% change

Physical limit: $G_S = -380$

10% change

$m_\pi^2 = 2 m_{phys}^2$: $G_S = -343 \pm 15$

quoted error bar due to uncertainty in m_q dependence in g_A



Dependence of binding energy on pion mass

Recall: Large scalar contribution

$$\frac{\text{B.E.}}{A} = -(120 - \frac{97}{A^{1/3}})\eta_s + (67 - \frac{57}{A^{1/3}})\eta_v + \text{residual terms}$$

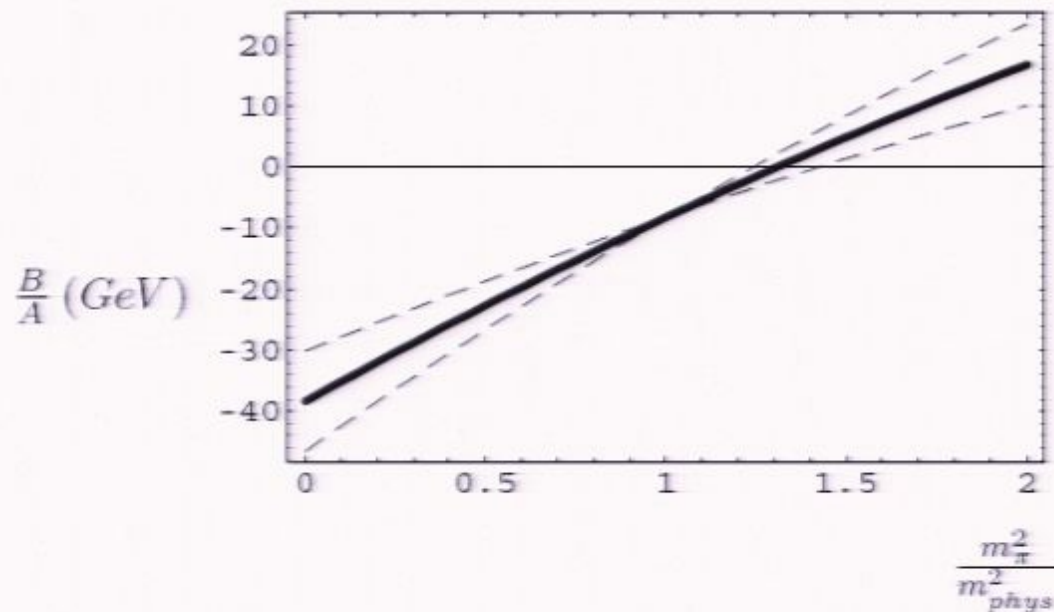
Cancellation amplifies relative effect:

$${}^{208}\text{Pb}: \quad \frac{\text{B.E.}}{A} = [-8 + 12.2 \frac{m_\pi^2 - m_{ph}^2}{m_{ph}^2}] \text{ MeV}$$

In general:

$$\begin{aligned} \text{Total B.E.} &= B(A) + (14.1A - 11.3A^{2/3}) \frac{m_\pi^2 - m_{ph}^2}{m_{ph}^2} \text{ MeV} \\ &\sim B(A) + (2.4A - 1.8A^{2/3})(\hat{m} - \hat{m}_{ph}) \end{aligned}$$

In a picture:



Note: Thibault Damour also produced a very nice treatment of nuclear matter in a Walecka model that provided an excellent understanding of the nuclear physics dependence of this calculation. It confirms the dominance of this particular coupling and says that the sub-dominant couplings enhance this effect.

Dependence of binding energy on pion mass

Recall: Large scalar contribution

$$\frac{\text{B.E.}}{A} = -(120 - \frac{97}{A^{1/3}})\eta_s + (67 - \frac{57}{A^{1/3}})\eta_v + \text{residual terms}$$

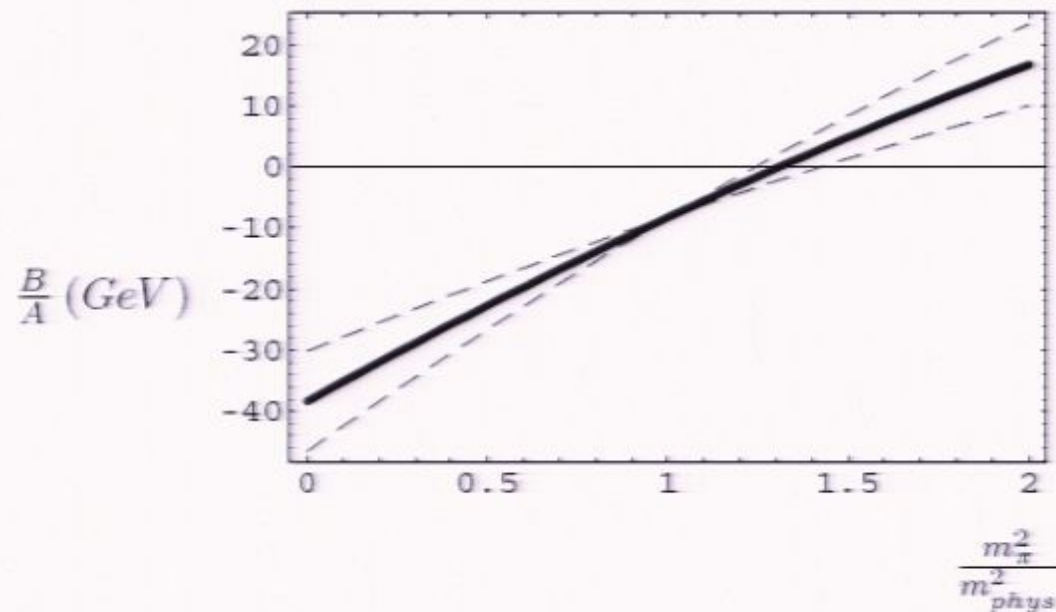
Cancellation amplifies relative effect:

$${}^{208}\text{Pb}: \quad \frac{\text{B.E.}}{A} = [-8 + 12.2 \frac{m_\pi^2 - m_{ph}^2}{m_{ph}^2}] \text{ MeV}$$

In general:

$$\begin{aligned} \text{Total B.E.} &= B(A) + (14.1A - 11.3A^{2/3}) \frac{m_\pi^2 - m_{ph}^2}{m_{ph}^2} \text{ MeV} \\ &\sim B(A) + (2.4A - 1.8A^{2/3})(\hat{m} - \hat{m}_{ph}) \end{aligned}$$

In a picture:



Note: Thibault Damour also produced a very nice treatment of nuclear matter in a Walecka model that provided an excellent understanding of the nuclear physics dependence of this calculation. It confirms the dominance of this particular coupling and says that the sub-dominant couplings enhance this effect.

Comment on strange quark dependence:

- no evidence that m_s plays significant role in nuclear binding
- maybe shift in Λ_{QCD}
- dispersive threshold is far away

$$G_{S,V} = \frac{2}{\pi} \int_{(2m_\pi, 3m_\pi)}^{\infty} \frac{d\mu}{\mu} \rho_{S,V}(\mu^2)$$

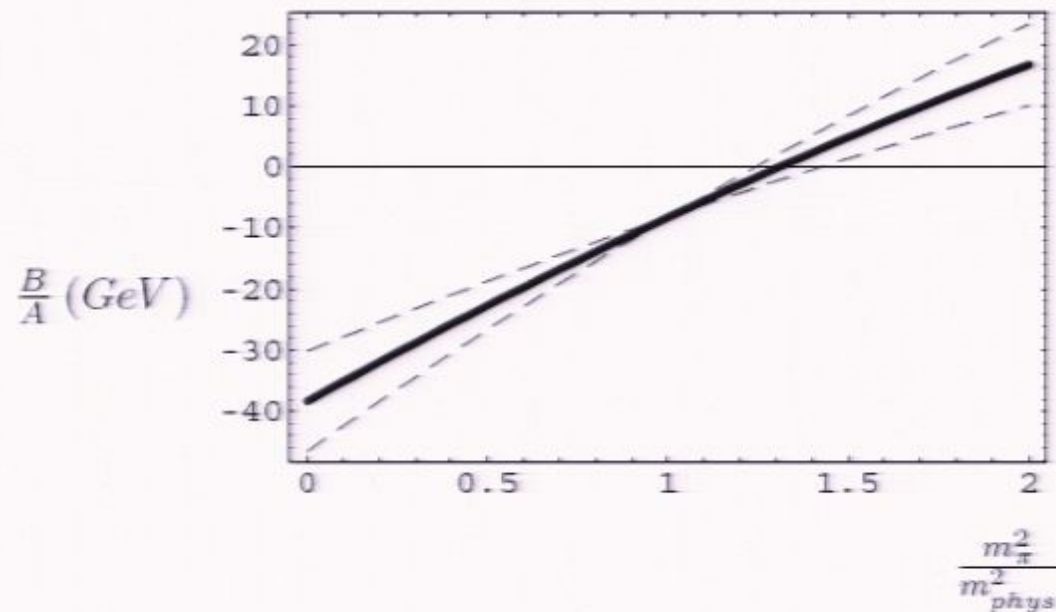

becomes $2m_K \sim 1 \text{ GeV}$

- dependence on mass gets **weaker** as the mass increases

But since constraint is really on $\Delta(m_q/\Lambda_{\text{QCD}})$

- there will be indirect effect from dependence of Λ_{QCD}
- but weaker

In a picture:



Note: Thibault Damour also produced a very nice treatment of nuclear matter in a Walecka model that provided an excellent understanding of the nuclear physics dependence of this calculation. It confirms the dominance of this particular coupling and says that the sub-dominant couplings enhance this effect.

Comment on strange quark dependence:

- no evidence that m_s plays significant role in nuclear binding
- maybe shift in Λ_{QCD}
- dispersive threshold is far away

$$G_{S,V} = \frac{2}{\pi} \int_{(2m_\pi, 3m_\pi)}^{\infty} \frac{d\mu}{\mu} \rho_{S,V}(\mu^2)$$


becomes $2m_K \sim 1 \text{ GeV}$

- dependence on mass gets **weaker** as the mass increases

But since constraint is really on $\Delta(m_q/\Lambda_{\text{QCD}})$

- there will be indirect effect from dependence of Λ_{QCD}
- but weaker

Anthropic constraints on quark masses:

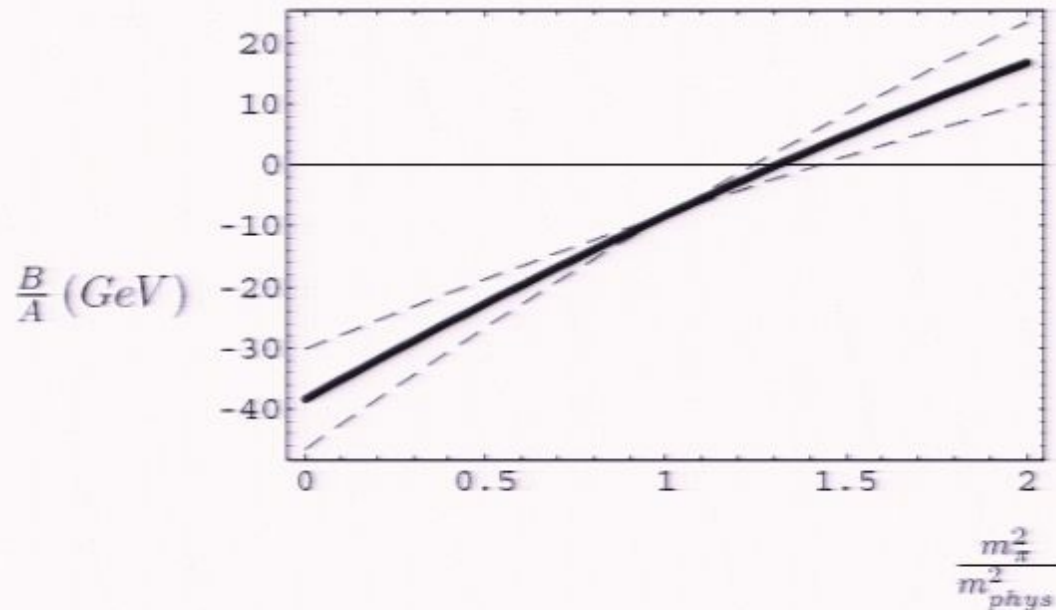
Damour
Donoghue

Basic constraint is **existence of atoms**:

Older work with
Agrawal
Barr
Seckel

- A) Changing quark masses can eliminate nuclear binding
- B) Summary of constraints

In a picture:



Note: Thibault Damour also produced a very nice treatment of nuclear matter in a Walecka model that provided an excellent understanding of the nuclear physics dependence of this calculation. It confirms the dominance of this particular coupling and says that the sub-dominant couplings enhance this effect.

Anthropic constraints on quark masses:

Damour
Donoghue

Basic constraint is **existence of atoms**:

Older work with
Agrawal
Barr
Seckel

- A) Changing quark masses can eliminate nuclear binding
- B) Summary of constraints

Comment on strange quark dependence:

- no evidence that m_s plays significant role in nuclear binding
- maybe shift in Λ_{QCD}
- dispersive threshold is far away

$$G_{S,V} = \frac{2}{\pi} \int_{(2m_\pi, 3m_\pi)}^{\infty} \frac{d\mu}{\mu} \rho_{S,V}(\mu^2)$$

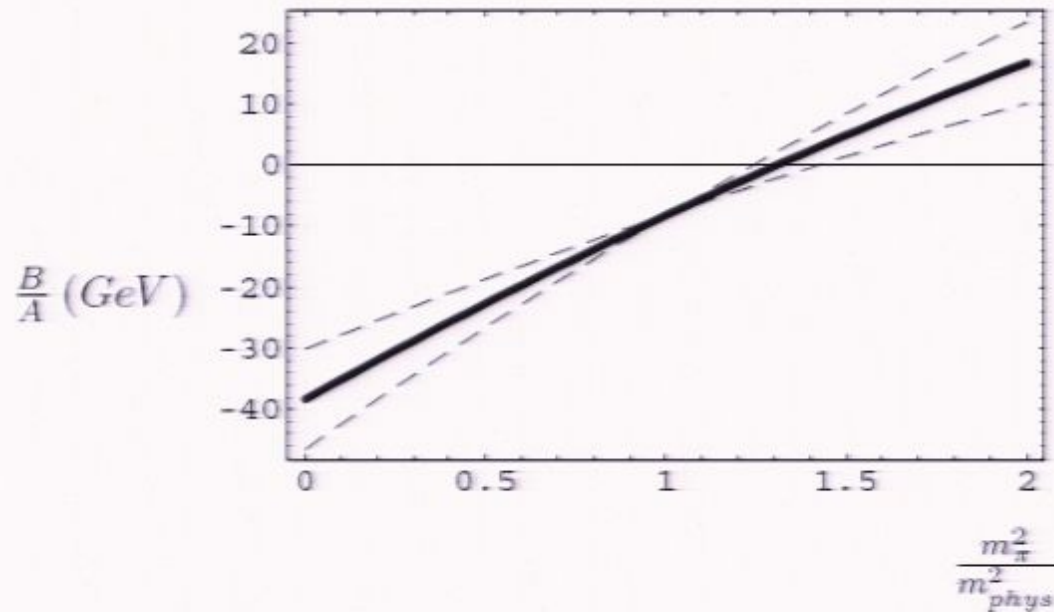
becomes $2m_K \sim 1 \text{ GeV}$

- dependence on mass gets **weaker** as the mass increases

But since constraint is really on $\Delta(m_q/\Lambda_{\text{QCD}})$

- there will be indirect effect from dependence of Λ_{QCD}
- but weaker

Nuclear binding only occurs for light quark masses:



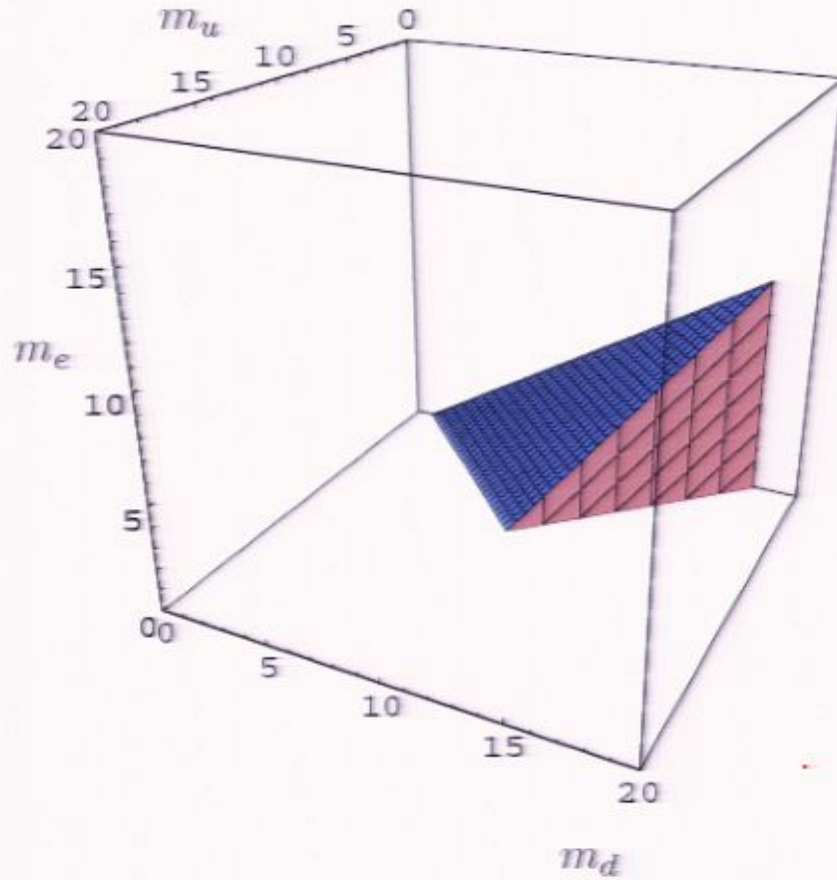
Anthropic constraint – existence of atoms

$$\frac{m_u + m_d}{(m_u + m_d)_{phys}} < 1.36 \pm 0.14$$

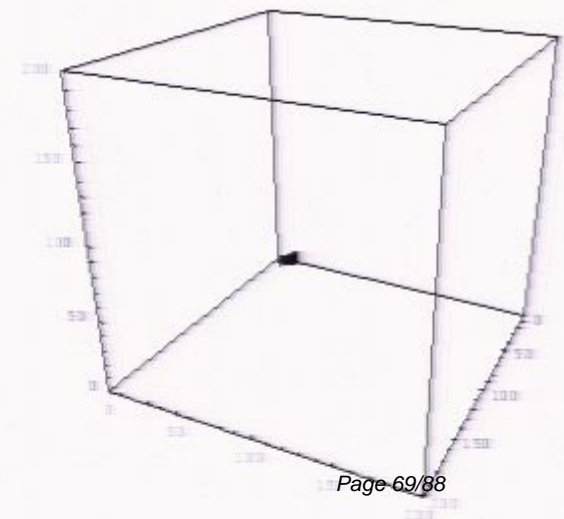
At 95% C.L. \rightarrow $\frac{m_u + m_d}{(m_u + m_d)_{phys}} < 1.64$ or

$$m_u + m_d \leq 18 \text{ MeV}$$

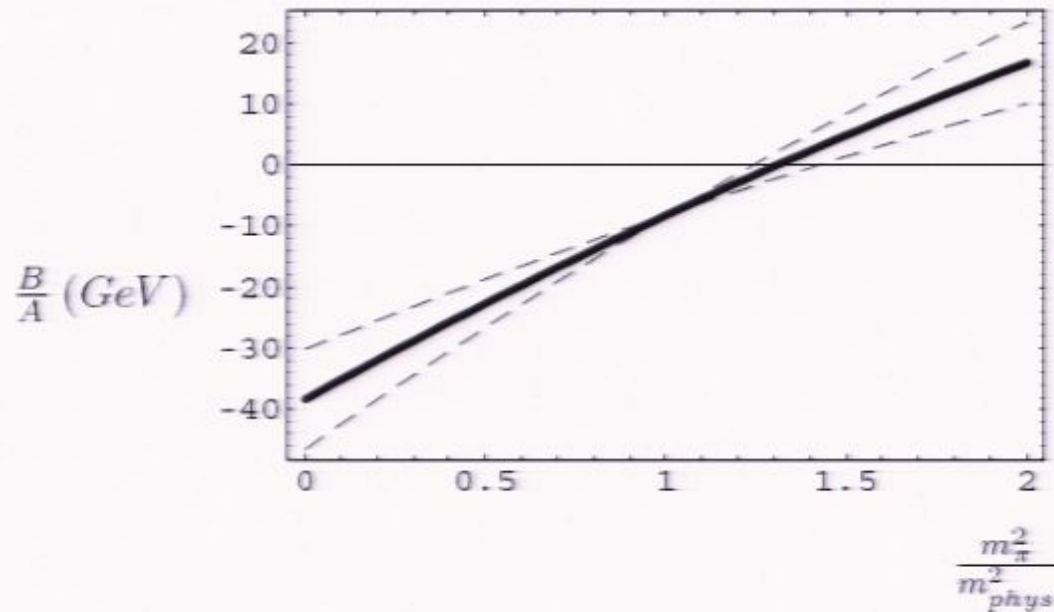
Overall constraints:



On the scale of Λ_{QCD}



Nuclear binding only occurs for light quark masses:



Anthropic constraint – existence of atoms

$$\frac{m_u + m_d}{(m_u + m_d)_{phys}} < 1.36 \pm 0.14$$

At 95% C.L. \rightarrow $\frac{m_u + m_d}{(m_u + m_d)_{phys}} < 1.64$ or

$$m_u + m_d \leq 18 \text{ MeV}$$

Anthropic constraints on quark masses:

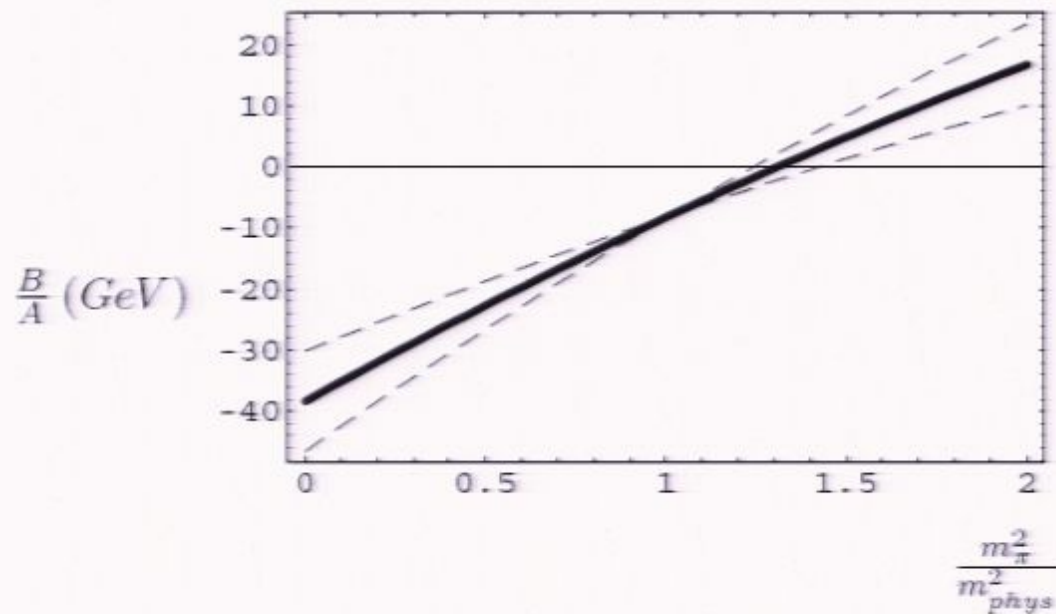
Damour
Donoghue

Basic constraint is **existence of atoms**:

Older work with
Agrawal
Barr
Seckel

- A) Changing quark masses can eliminate nuclear binding
- B) Summary of constraints

Nuclear binding only occurs for light quark masses:



Anthropic constraint – existence of atoms

$$\frac{m_u + m_d}{(m_u + m_d)_{phys}} < 1.36 \pm 0.14$$

At 95% C.L. \rightarrow $\frac{m_u + m_d}{(m_u + m_d)_{phys}} < 1.64$ or

$$m_u + m_d \leq 18 \text{ MeV}$$

Second Anthropic constraint:

- atoms do not decay into neutron world

$$m_P + m_e \leq m_N$$

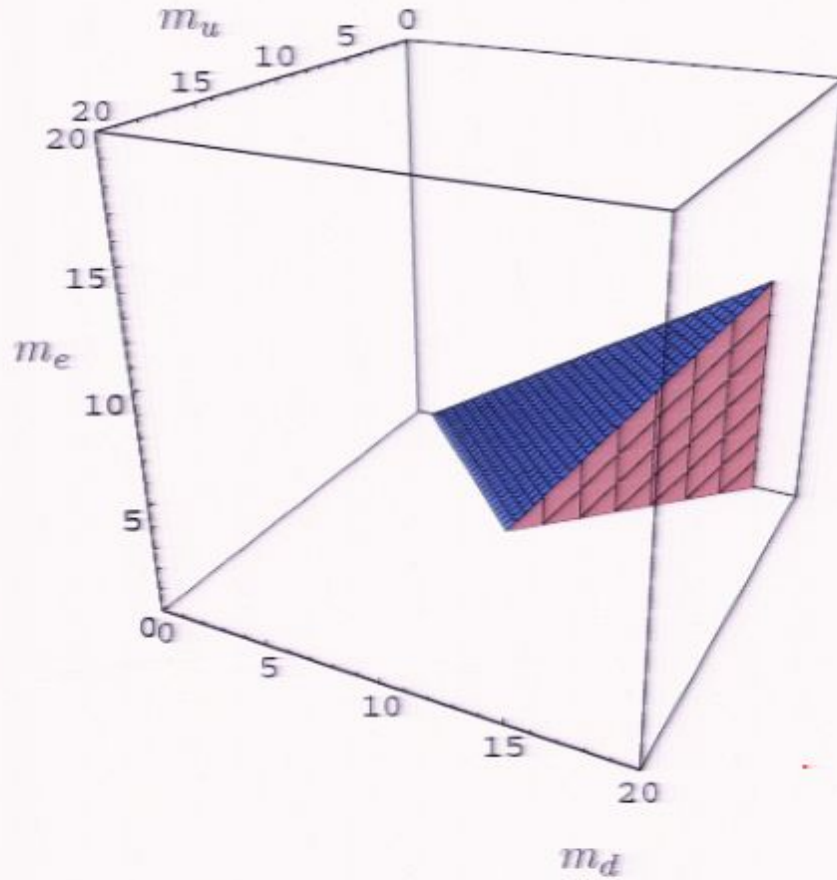
Here we need to account for E&M also:

$$m_N - m_P = Z_0(m_d - m_u) - \epsilon_{EM}$$

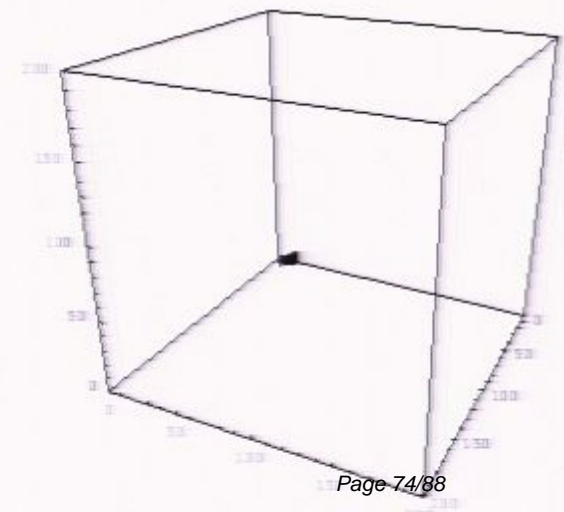
My estimates:

$$m_d - m_u - 1.6m_e \geq 0.85 \text{ MeV}$$

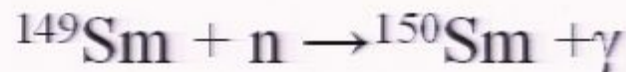
Overall constraints:



On the scale of Λ_{QCD}



Oklo constraint – time variation of quark masses



Shlyakhter
Damour, Dyson

$$-0.12 \text{ eV} < \Delta(Q - E_*) < 0.09 \text{ eV}$$

Very roughly:

- estimate $\Delta Q \sim \eta \Delta \langle V \rangle_1$ with $\eta \sim 1/2$
- with previous work, translates to

$\eta=1$ is result
of Flambaum
and Shuryak

$$\frac{|\Delta m_q|}{m_q} \leq 2 \times 10^{-8}$$

over a time scale of 1.8×10^9 yrs

or
$$\frac{|\dot{m}_q|}{m_q} \leq 3.6 \times 10^{-25} \text{ sec}^{-1}$$
 if linear

Aside: Strongest constraint on time variation:

- Assumption – Cosmological constant has not varied by more than 100% since $z \sim 1$ ($\sim 8 \times 10^9$ yrs)
- agreement of CMB and supernova data
- non-closure of universe
- will be refined

$$\Lambda = \Lambda_0 + m_q B_0 + m_q^2 C_0 + \dots$$

- Consider **only** quark mass variation
 - only first order term linear in the quark mass – **rigorous**

$$\Delta\Lambda = \left(\frac{\Delta m_\pi^2}{m_\pi^2} \right) F_\pi^2 m_\pi^2 = \left(\frac{\Delta m_q}{m_q} \right) \times (112 \text{ MeV})^4$$

Result:

$$\frac{|\Delta m_q|}{m_q} \leq 1.7 \times 10^{-43} \quad \text{or} \quad \frac{|\dot{m}_q|}{m_q} \leq 7 \times 10^{-61} \text{ sec}^{-1}$$

Application to equivalence principle tests:

- our original motivation for getting into this topic
- B.E. contribution is least understood ingredient

Scalar couplings:

$$\phi \bar{\psi} \psi \quad \text{like} \quad m \bar{\psi} \psi$$

Leading quark mass effect is in the masses of nucleons

- reasonably well understood

EP tests compare acceleration of different elements

- need to compare BE for different elements

Generic scalar models

Coupling to any scalar invariant:

-generally suppressed by powers of some heavy mass

$$S = \int d^4x \sqrt{g} \left[\frac{B_g(\phi)}{16\pi G} R - \frac{k}{4} B_F(\phi) F^2 - B_m(\phi) m \bar{\psi} \psi + \dots \right]$$

Specific models have predictions for the couplings

Two sample physical consequences:

- 1) All violate the equivalence principle at some level
- 2) If ϕ changes in time, the coupling constants change

Differences in acceleration

With massless scalar:

$$G_{AB} = G(1 + \alpha_A \alpha_B)$$

with

$$\alpha_A = \frac{1}{m_A} \frac{\partial m_A}{\partial \phi}$$

Then: $\left(\frac{\Delta a}{a}\right)_{AB} \equiv 2 \frac{a_A - a_B}{a_A + a_B} \simeq (\alpha_A - \alpha_B) \alpha_E$

But if all energies proportional to Λ_{QCD} , then α_i universal
- need to know contributions of quark masses and EM

Example – runaway dilaton (ignoring quark masses)

$$\left(\frac{\Delta a}{a}\right)_{AB} \simeq 2 \times 10^{-5} \alpha_{\text{had}}^2 \left[\left(\frac{E}{M}\right)_A - \left(\frac{E}{M}\right)_B \right] \quad E \equiv Z(Z-1)/(N+Z)^{1/3}$$

What is missing?

Reasonable understanding of:

- Quark mass effects on nucleons
- EM effects on nucleons
- EM in nuclear binding

$$m_p = m_\Lambda + b_u m_u + b_d m_d + C_p \alpha$$

$$m_n = m_\Lambda + b_d m_u + b_u m_d + C_n \alpha$$

$$m(\text{Atom}) = Zm_p + Nm_n + Zm_e + E_3 + E_1$$

↑ ↗
QCD EM

Missing:

- Quark mass effects on nuclear binding $E_3 = E_\Lambda + E_m$

⇒ Need to understand

$$\frac{\partial E_3}{\partial m}$$

The dependence on Nuclear number:

Pair interactions depend on near neighbors:

- nuclear density nearly constant in central region $r \sim A^{1/3}$

- central interactions $\# \sim r^3 \sim A = \#$ of nucleons

- surface interaction correction $\sim r^2 \sim A^{2/3}$

$$B.E. \sim a(A - bA^{2/3})$$

(like semi-empirical mass formula)

fits give $b \sim 1$

predicts nuclear matter limit to 6%

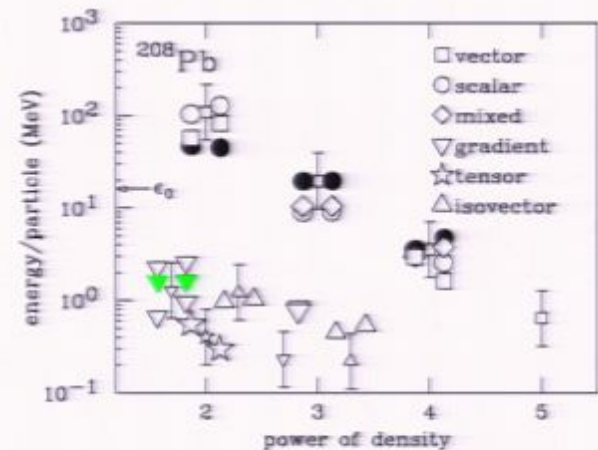
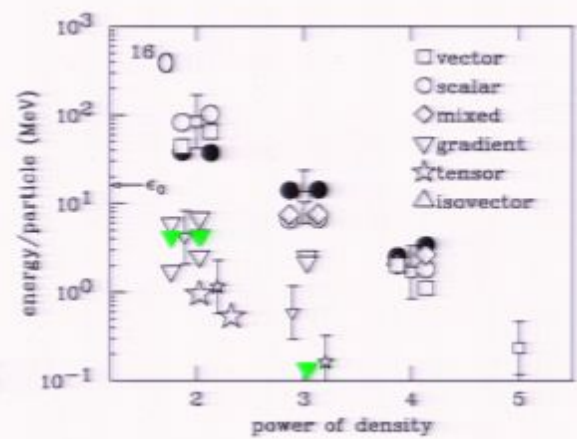


FIG. 2. Same as Fig. 1 for ^{208}Pb .
Page 81/88

Qualitative conclusion:

- B.E. differences not large in EP tests
- reason is clear

For most test materials, BE per nucleon is roughly constant
BE contribution then roughly proportional to mass
quark mass dependence shares this property
then – scalar coupling to BE roughly proportional to mass

- details to be forthcoming

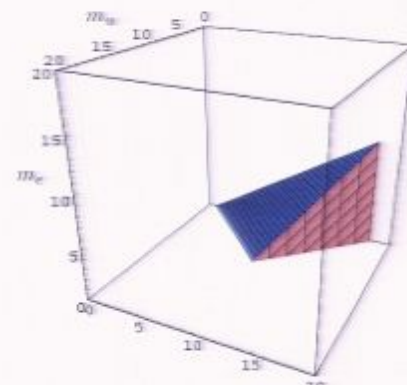
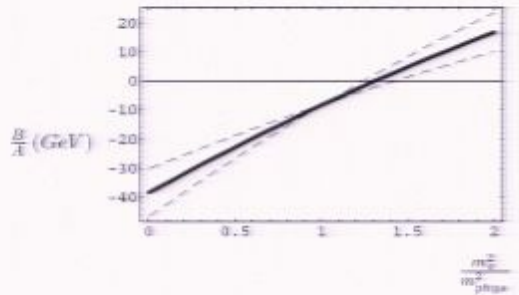
Summary

Reasonable control over the key ingredient in nuclear binding

Quark mass dependence comes from region where the calculation is the most reliable

Reasons for strong dependence are well understood

Applications to:
Anthropics
Oklo
Equivalence Principle
.....



The dependence on Nuclear number:

Pair interactions depend on near neighbors:

- nuclear density nearly constant in central region $r \sim A^{1/3}$
- central interactions $\# \sim r^3 \sim A = \#$ of nucleons
- surface interaction correction $\sim r^2 \sim A^{2/3}$

$$B.E. \sim a(A - bA^{2/3})$$

(like semi-empirical mass formula)

fits give $b \sim 1$

predicts nuclear matter limit to 6%

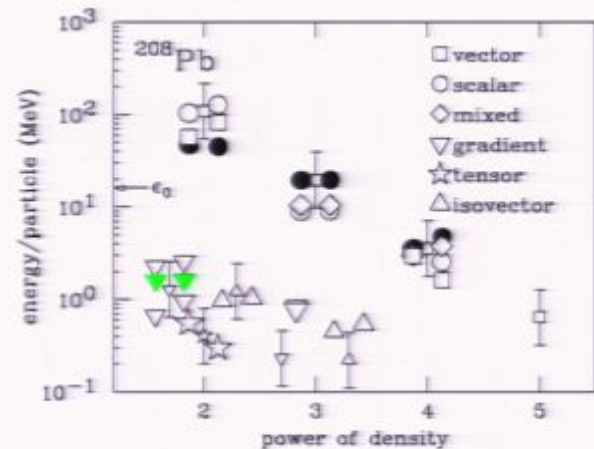
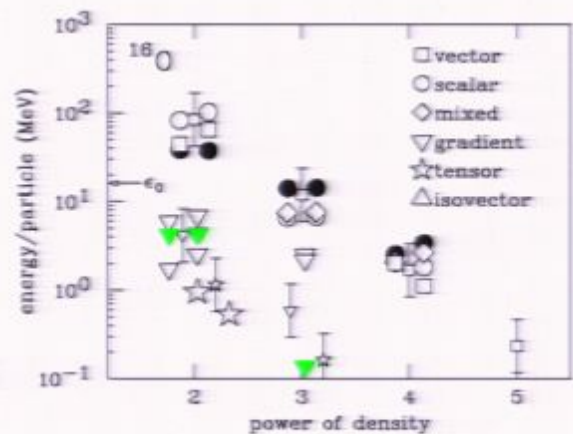


FIG. 2. Same as Fig. 1 for ^{208}Pb .
Page 84/88

What is missing?

Reasonable understanding of:

- Quark mass effects on nucleons
- EM effects on nucleons
- EM in nuclear binding

$$m_p = m_\Lambda + b_u m_u + b_d m_d + C_p \alpha$$

$$m_n = m_\Lambda + b_d m_u + b_u m_d + C_n \alpha$$

$$m(\text{Atom}) = Zm_p + Nm_n + Zm_e + E_3 + E_1$$

↑ ↗
QCD EM

Missing:

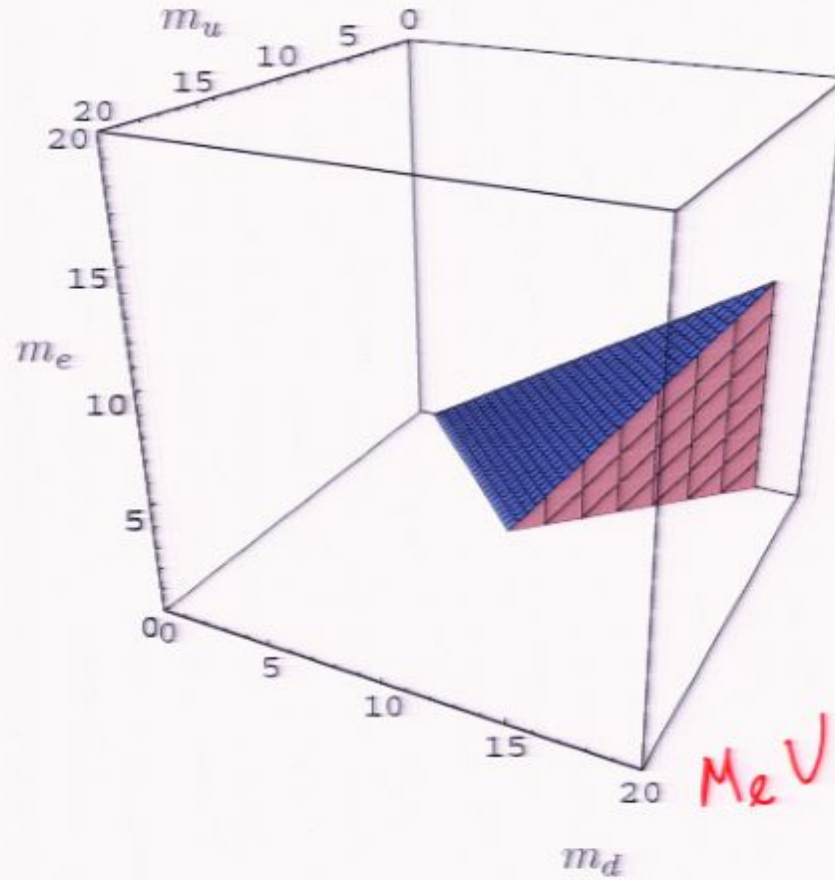
- Quark mass effects on nuclear binding

$$E_3 = E_\Lambda + E_m$$

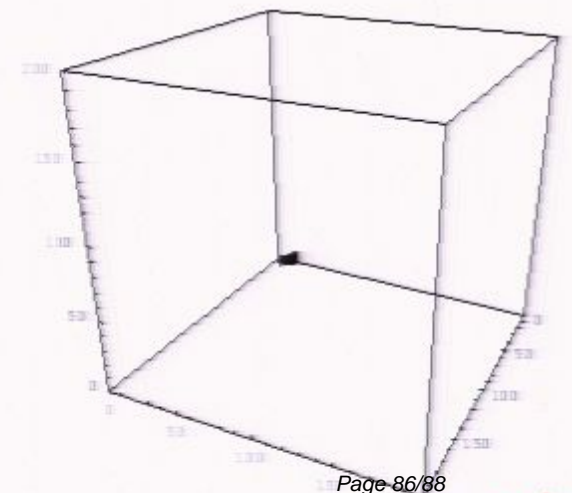
⇒ Need to understand

$$\frac{\partial E_3}{\partial m}$$

Overall constraints:



On the scale of Λ_{QCD}



Comment on strange quark dependence:

- no evidence that m_s plays significant role in nuclear binding
- maybe shift in Λ_{QCD}
- dispersive threshold is far away

Dependence of binding energy on pion mass

Recall: Large scalar contribution

$$\frac{\text{B.E.}}{A} = -(120 - \frac{97}{A^{1/3}})\eta_s + (67 - \frac{57}{A^{1/3}})\eta_v + \text{residual terms}$$

Cancellation amplifies relative effect:

$${}^{208}\text{Pb}: \quad \frac{\text{B.E.}}{A} = [-8 + 12.2 \frac{m_\pi^2 - m_{ph}^2}{m_{ph}^2}] \text{ MeV}$$

In general:

$$\begin{aligned} \text{Total B.E.} &= B(A) + (14.1A - 11.3A^{2/3}) \frac{m_\pi^2 - m_{ph}^2}{m_{ph}^2} \text{ MeV} \\ &\sim B(A) + (2.4A - 1.8A^{2/3})(\hat{m} - \hat{m}_{ph}) \end{aligned}$$